Diagnostic efficacy of dynamic liver imaging using qualitative diagnostic algorithm versus LI-RADS v2018 lexicon for atypical versus classical HCC lesions: A decade of experience from a tertiary liver institute

Shalini Thapar Laroia[a,*], Komal Yadav[a], Archana Rastogi[b], Guresh Kumar[c], Senthil Kumar[d], Shiv Kumar Sarin[e]

[a] Department of Radiology, Institute of Liver and Biliary Sciences, Sector D-1, Vasant Kunj, New Delhi, 110070, India
[b] Department of Pathology, Institute of Liver & Biliary Sciences, Sector D-1, Vasant Kunj, New Delhi, 110070, India
[c] Department of Research, Institute of Liver & Biliary Sciences, Sector D-1, Vasant Kunj, New Delhi, 110 070, India
[d] Department of HPB Surgery and Liver Transplantation, Institute of Liver & Biliary Sciences, Sector D-1, Vasant Kunj, New Delhi, 110 070, India
[e] Chair of Department of Hepatology, Institute of Liver & Biliary Sciences, Sector D-1, Vasant Kunj, New Delhi, 110070, India

ARTICLE INFO

ABSTRACT

Objective: To analyze and evaluate the diagnostic performance of conventional diagnostic (qualitative) imaging features versus LI-RADSv2018 lexicon for indeterminate and atypical Hepatocellular carcinoma (HCC) on dynamic liver imaging with reference to histopathology.

Patients and methods: This retrospective study (June 2009–June 2019) evaluated the performance characteristics of conventional imaging findings, versus the Liver Imaging Reporting and Data System (LIRADS) v2018, for interpretation of indeterminate and atypical HCC, in patients who underwent subsequent histopathological analysis (gold standard). A total of 100,457 dynamic hepatobiliary CT and MR examinations were performed over ten years at our institute. Using current international imaging guidelines, 3218 patients were found to have suspected liver cancer lesions on imaging. Classical enhancement pattern of typical HCC was seen in 2916 of these patients. These patients did not require further biopsy. We enrolled, the remaining (n = 302) patients, who underwent biopsy, into our study group. Two radiologists, blinded to pathology findings, reviewed and classified these lesions, in consensus, according to LI-RADS® lexicon and as per 'conventional' (Indeterminate, Atypical HCC, Classical HCC, other malignancies) imaging. The histopathology diagnosis was considered as the final diagnosis. Alpha feto protein (AFP) levels amongst various subgroups were compared. Statistical analysis was performed to calculate the efficacy of LIRADS versus qualitative imaging parameters in comparison with histopathology.

Results: A total of n = 302 patients, [89 % men (n = 269), mean age 57.08 ± 12.43 years] underwent biopsy for suspected liver lesions. Qualitative imaging had 92.3 % (CI 88.53–94.91) sensitivity, 41.4 % (CI 25.51–59.26) specificity, positive predictive value (PPV) of 93.7 % (CI 90.11–96.02), negative predictive value (NPV) of 36.4 % (CI 22.19–53.38), positive likelihood ratio (PLHR) of 1.575 (CI 1.40–1.77) and negative likelihood ratio of (NLHR) 0.19 (CI 0.13-0.26). It correctly classified 87.4 % of lesions diagnosed on pathology. In comparison, LI-RADS was found to have 92 % sensitivity, 55.5 % specificity, 97 % PPV, 30.3 %, NPV, PLHR 2.068 (CI 1.62–2.64), NLHR 0.15 (CI 0.11-0.18) and 89.7 % diagnostic accuracy. A total of 38 patients (17 false negative, 21 false positive lesions) had discordant diagnoses on imaging versus histopathology. The kappa agreement between LIRADs and qualitative Imaging was found to be 0.77 ± .07 (p < 0.001). LIRADS and qualitative imaging collectively had 97 % sensitivity, 30 % specificity, 91.9 % PPV, 55.6 % NPV, PLHR of 1.39 (CI 1.27–1.51) and NLHR of 0.09 (0.048-0.19) which was better than, either reporting system, independently.

Conclusion: It was observed that the LI-RADS v2018 lexicon with qualitative imaging as a combination technique added extra value in interpretation of atypical HCC or indeterminate lesions on dynamic CT and MRI compared to either as 'stand- alone' reporting systems.

---

* Corresponding author.
E-mail addresses: thaparshalini@gmail.com (S.T. Laroia), komal.yleo@gmail.com (K. Yadav), drarchanarastogi@gmail.com (A. Rastogi), chibbegk@gmail.com (G. Kumar), sanskrity@hotmail.com (S. Kumar), shivsarin@gmail.com (S.K. Sarin).

1. Introduction

1.1. Background

Hepatocellular carcinoma (HCC) is currently, the sixth most common malignancy, globally [1,2]. The international epidemiology statistics, last published in 2012, stated that almost 700,000 new HCC patients were diagnosed annually throughout the world [3]. The bulk of these patients belong to developing countries in Asia and Africa, followed closely by the western population [4]. The crux of managing the disease burden of this magnitude lies on an early accurate diagnosis, for which imaging is the key. Patients are more likely to receive curative therapy such as Liver transplantation or radiofrequency ablation if diagnosed promptly. There are clear-cut guidelines in place for the surveillance and screening of patients at risk of HCC such as with underlying Hepatitis B (HBV) or C virus infection (HCV) as well as patients with metabolic syndrome or non-alcoholic fatty liver disease (NAFLD). Imaging plays an important role in the surveillance and follow-up of suspicious lesions diagnosed during the disease course amongst the population at risk.

The diagnosis of HCC is predominantly made with the help of imaging modalities such as Computed tomography (CT) and Magnetic
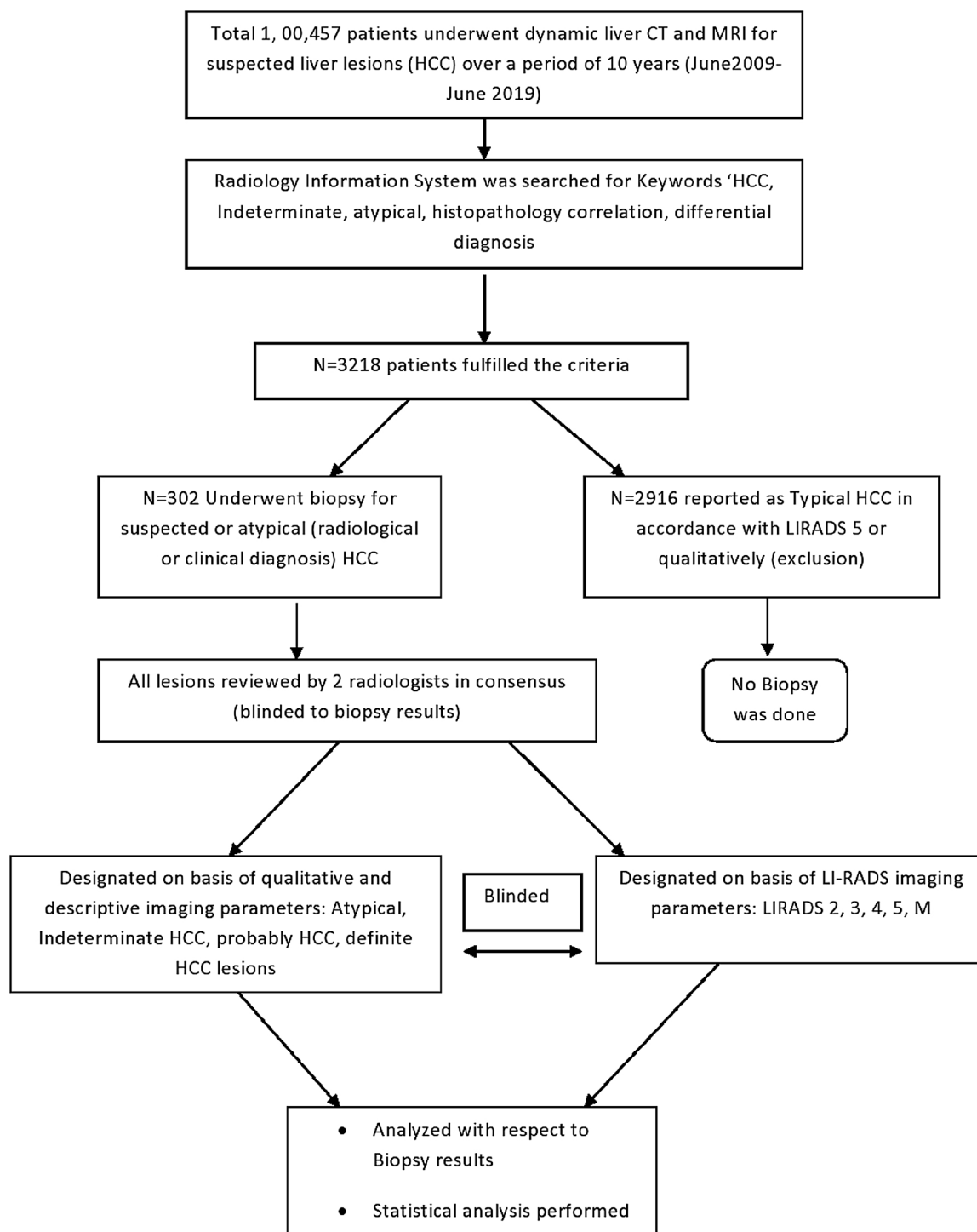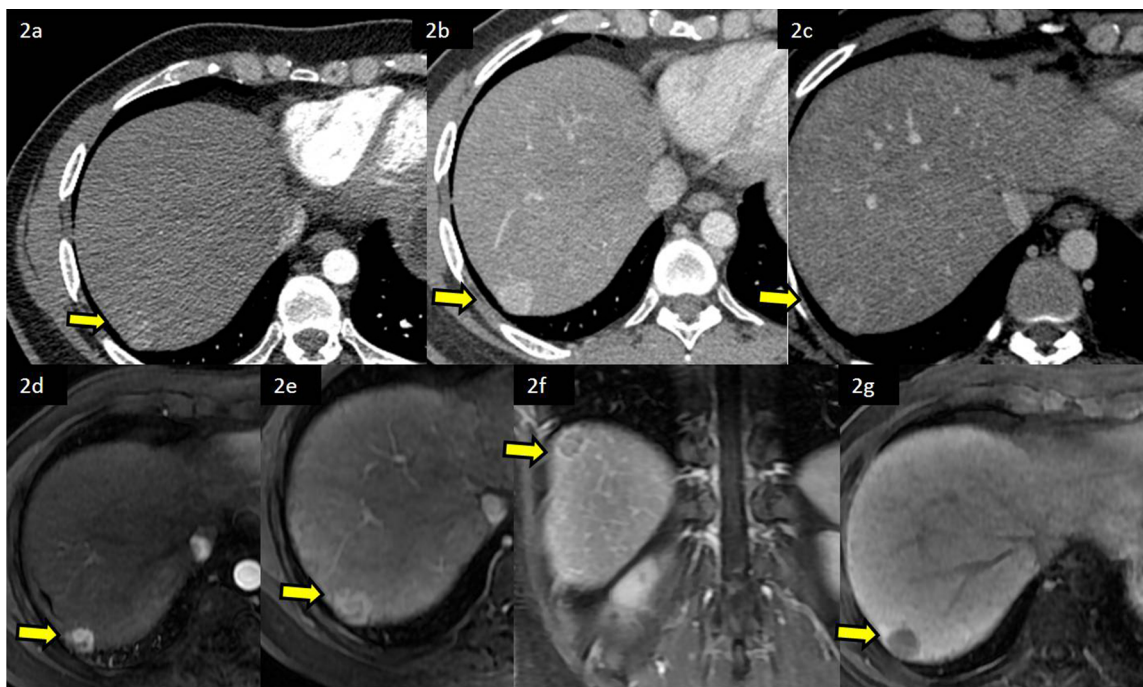

Fig. 1. Study Design.

Fig. 2. Dynamic contrast enhanced CT(CECT) and MRI (CEMRI)scans showing the same liver lesion with enhancement pattern characteristic of classical HCC (2a). Axial section of CECT scan of the liver in hepatic arterial phase (HAP) showing well defined sub capsular hypervascur lesion (bold arrow) in segment VII. (2b). Lesion in segment VII shows non rim enhancement (arrow) on early portal venous phase (PVP) with (2c.)central washout (arrow) on equilibrium phase (2d.)CEMRI, axial section of the liver shows better lesion delineation with non-rim hypervascularity on HAP (arrow) (2e.) Lesion shows mild central washout on PVP (arrow) with (2f.) Capsule formation and central washout (arrow) on coronal equilibrium phase. (2 g.) Lesion is seen as signal defect with hypointense area on delayed 1 h hepatobiliary phase (arrow).
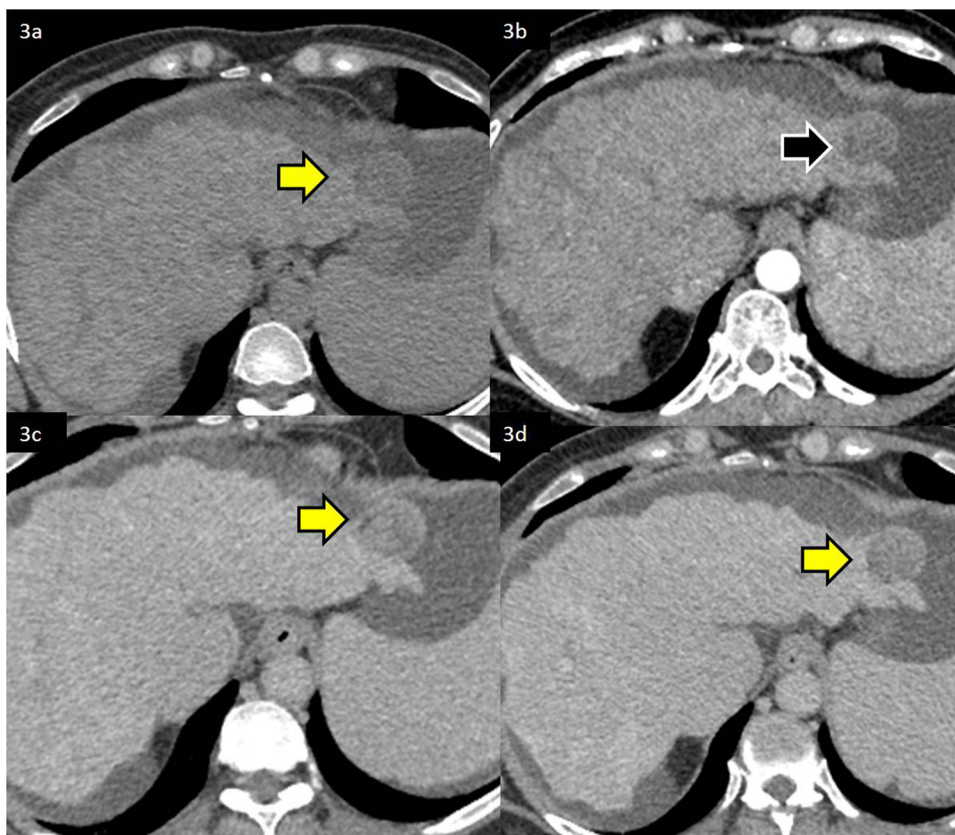
Fig. 3. Dynamic CECT scan of a patient with liver cirrhosis showing enhancement pattern (diagnosis on qualitative imaging, later corroborated on biopsy) of hypovascular HCC.
(3a.) Non-contrast axial section of the liver with lobulated nodular cirrhosis pattern showing a n exophytic rounded (arrow) hypoattenuating lesion in segment II a. (3b.) Lesion shows no enhancement (arrow) on HAP (3c, d) Subsequent PVP and equilibrium phases show partially enhanced soft tissue within the hypodense lesion (arrow) with well-defined capsule formation.
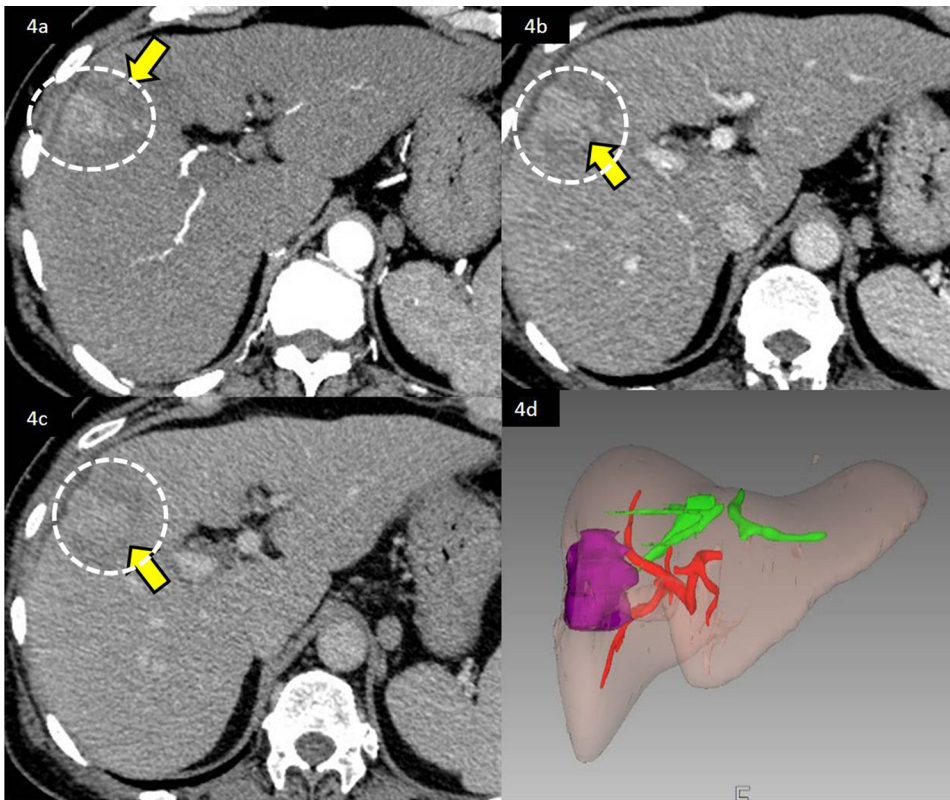
Fig. 4. Dynamic CECT scan of a patient with liver cirrhosis showing enhancement pattern of combined Hepatocholangiocarcinoma (diagnosis made on qualitative imaging, later corroborated on biopsy).

(4a.)axial section of CECT ill-defined area of hypervascularity on HAP (dotted circle) within a subcapsular lesion in segment V (arrow) of liver (4b.)Inferior portion of the lesion shows washout, whereas the superior segment (4c) shows progressive enhancement (4d) Volumetry software used to depict the volume of lesion for planning further segmentectomy (lesion in pink).

resonance imaging (MRI) with only a limited role of histopathology in select cases where the classical findings of arterial hypervascularity followed by washout are not present. Working algorithms for surveillance and diagnosis of HCC have been described by various associations worldwide, namely, the European Association for the Study of the Liver (EASL), Asian-Pacific Association for the Study of Liver (APASL) and the American Association for the Study of Liver disease (AASLD) [5,6].

In the recent years, several studies have described the application of standardized lexicons and algorithms such as LI-RADS (latest version v2018) for uniformity of reporting lesions seen during the course of surveillance and screening of HCC [7]. Newer techniques (3 Tesla MRI systems, diffusion weighted sequence, spectral CT scanners, high resolution and contrast ultrasound) and better contrast agents (such as hepatocyte specific agents in MRI and high iodine density non-ionic molecules in CT) have augmented the specificity and predictive accuracy of imaging for diagnosis of early or well differentiated HCC, smaller tumors and atypical lesions such as dysplastic nodules [8].

Existing diagnostic criteria for classification of atypical or classical HCC nodules as well as the spectrum of nodules seen during hepatocarcinogenesis have been described exclusively in cirrhotic patients. The American College of Radiology (ACR) has updated the LI-RADS version recently in 2018 and integrated it with the AASLD practice guidelines for HCC [9]. In the current (v. 2018) LI-RADS, the diagnosis of HCC is based on the presence of major and ancillary features with a modification in LR 5 category observations. The current version has been simplified and does not require the lesion in LR5 category to be visualized before the CT or MRI study by an ultrasound [7].

Few studies in literature have reported the comparison of diagnostic performance of conventional radiological reporting versus the Liver Imaging Reporting and Data System (LI-RADS) in the diagnosis of atypical hepatocellular carcinoma or indeterminate lesions with respect to the histopathological findings. We reviewed the literature and found an existing lacuna regarding studies using LIRADS for observations which were non-classical or atypical in nature and are hence placed in LR3, LR4 or LR M categories. No previous study has been done, to the

best of our knowledge, comparing the accuracy of conventional radiology reporting versus the LI-RADS lexicon in characterization of atypical HCC, indeterminate nodules or other malignancies in patients with chronic liver disease with reference to a gold standard of histopathology.

This study assessed the spectrum of uncorroborated atypical, indeterminate and various other lesions, observed over a course of ten years on dynamic CT and MRI which were later confirmed on histopathology. Subsequently, we reviewed these lesions using both conventional radiology reporting and LI-RADS lexicon. We compared the performance characteristics of the two methods of observation, from a radiologist's perspective of suspected HCC or indeterminate nodules in the liver with respect to biopsy results, as the gold standard.

2. Patients and methods

2.1. Patients

Our institutional review board approved this retrospective study with a waiver for the informed consent requirement. The prospectively maintained and electronically searchable, radiology information system database of a period of ten years (June 2009- June 2019) was searched for all patients with underlying chronic liver disease, who underwent a four phase dynamic hepatic CT and/or hepatobiliary specific contrast enhanced MRI scans (n = 1,00,457) with the following keywords as search criteria: "Hepatocellular carcinoma"(HCC) "atypical HCC", "indeterminate lesions", "histopathology correlation", "differential diagnosis HCC" (total number, n = 3218). The collected database was then segregated into patients who underwent histopathology evaluation in the form of lesion biopsy or surgical resection followed by pathology analysis (n = 302) and those who did not require biopsy due to classical HCC characteristics on imaging (typical arterial phase enhancement followed by subsequent washout) (n = 2916). The following inclusion criteria were applied: The biopsy and histopathological analysis was performed within four weeks of imaging: No history of previous
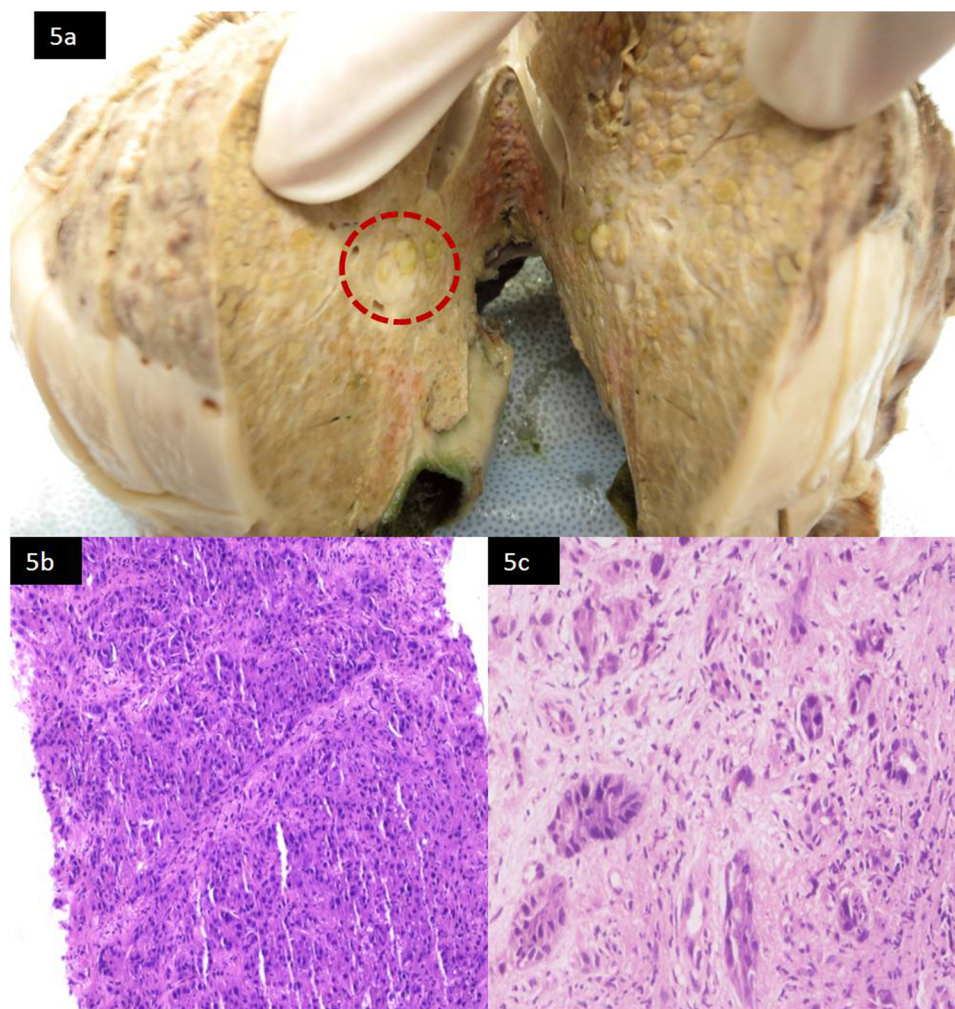
Fig. 5. Gross (5a) and microscopic histopathology (5b, c) of the combined HCC-Cholangiocarcinoma, tumor seen as a nodule (dotted red circle).

therapy was present in the study group. Imaging by CT and MRI were performed as per institutional standardized protocol for dynamic liver studies.

A total of 302 patients who underwent biopsy and histopathology evaluation (including 262 confirmed cases of HCC) [269 (89 %) men, mean age of 57.1 ± 12.4 years] were included. In all observations, LI-RADS v2018 and qualitative assessment was made independently.

2.2. Study design

This was a retrospective, single center study over a ten-year period (2009–2019). The study design has been depicted in the (Fig. 1).

2.3. Image acquisition

2.3.1. Multi detector computed tomography (MDCT)

All CT studies were performed with the triple phase dynamic liver imaging protocol using multi-detector, spectral CT scanner (Discovery 750HD, 64 slices, GE, GE Healthcare, USA). For intravenous contrast, nonionic contrast material Iomeron 400 (Iopomerol, Bracco, Milano, Italy) was injected after calculating the dose at 1.5 mL/kg body weight (total volume < 150 ml) using power injector (Medrad, Pittsburgh, PA, USA) and bolus tracking technique. Non-contrast scan was obtained before the administration of contrast media. Bolus tracking was done and hepatic arterial phase imaging was acquired after an 18-second delay from the time 100 Hounsfield units of aortic enhancement was visualized. A 30-second scan delay was used for portal venous phase

imaging, after the arterial phase acquisition. Equilibrium phase imaging was also obtained 180 s after the beginning of injection. The scanning parameters followed were as below: 64-row spectral CT scanner, 120 kV with automated mA, 0.6 s rotation time, speed 55 mm/rotation, pitch of 1.375:1, detector coverage 40 mm, and matrix size of 512 × 512, section thickness 0.625 mm, collimation 16 rows x0.75 mm or 64 rows x0.6 mm; gantry rotation speed 0.625 s; image reconstruction (using reiterative techniques) increment, 1.25 mm; 120 kV; and effective tube current-time charge, 120 mA.

2.3.2. Magnetic resonance imaging (MRI)

Magnetic resonance images were obtained using a 3 T MRI system (Signa HD xt 3 T Volume, GE, GE Healthcare, USA). The MRI protocol included all the parameters' specified by LI-RADS technical requirements. Pre-contrast sequences included gradient breath holdT1-weighted (T1-WI), in phase (IP) and out of phase (OP), breath-hold as well as respiratory gated, balanced steady-state gradient echo sequence (both coronal and axial planes), fat-saturated, T2-weighted, spin-echo sequence in both axial and coronal planes, diffusion weighted imaging with *b values* of 0, 800 and 1000 were obtained for all scans. Apparent diffusion coefficient maps were obtained with the help of automated software provided by the GE workstation incorporated in the scanner. The contrast-enhanced dynamic MR images were obtained after intravenous administration of Gadobenate dimeglumine (BOPTA) Multihance ; Bracco, Germany) administered at 0.025 mmol/kg of body weight at 2 mL/s. Hepatic arterial phase (HAP), portal venous phase (PVP) and delayed phase were obtained at 30, 60 and 180 s
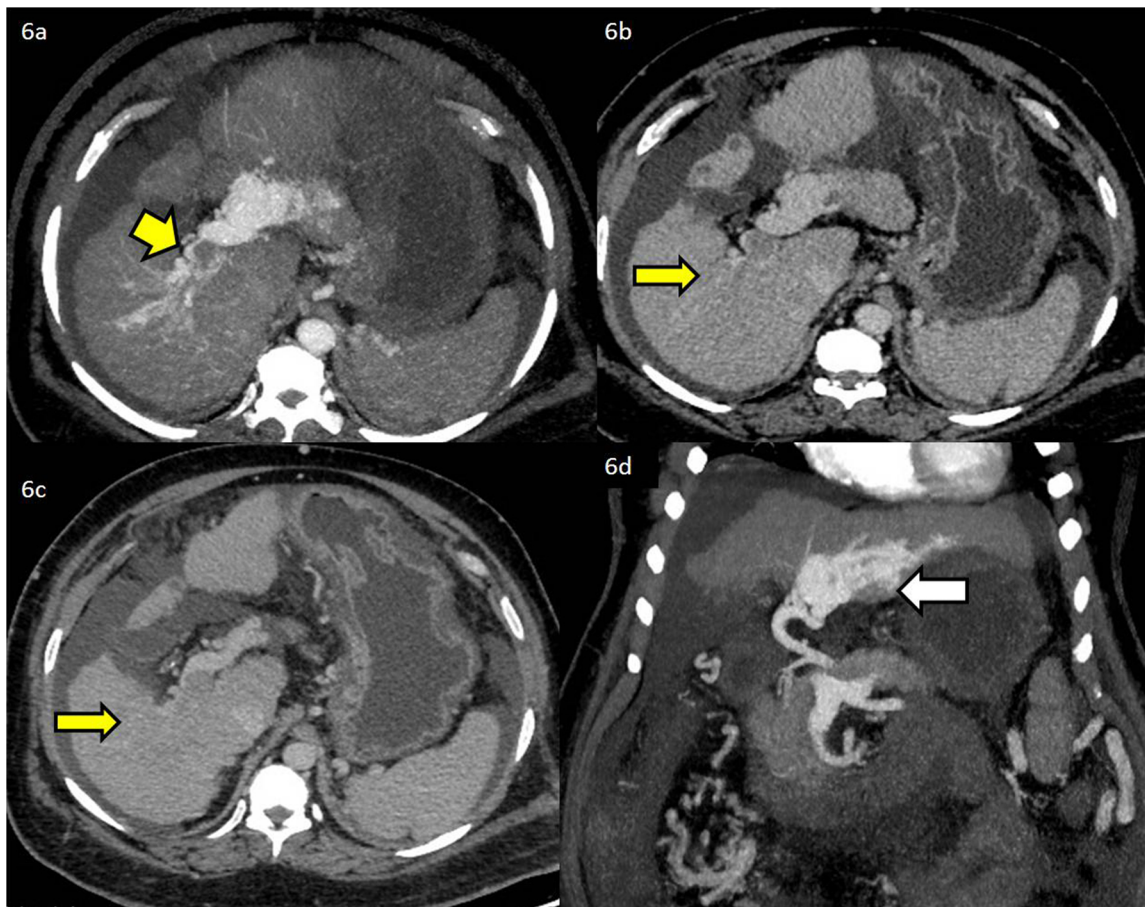
Fig. 6. Dynamic contrast enhanced CT scan of a patient with cirrhosis of liver showing features of ill visualized infiltrative- cirrhotomimic HCC enhancement pattern corresponding to LIRADS 4 observation.

(6a.)Axial section of contrast enhanced CT scan of the liver in hepatic arterial phase (HAP) showing ill defined areas of arterial vascularity (bold arrows) in segment VI and VII of liver (6b.) Lesion (arrow) is not visualized on PVP, instead there is a hypodense expansile thrombus in the right portal vein at the bifurcation (bold yellow arrow)(6c.) The area corresponding to the lesion in segment VI and VII shows mild hypoattenuation on equilibrium phase without obvious washout (6d) arterio-portal shunt is present along left portal vein (white arrow).

respectively, post injection. An extended hepatobiliary phase scan was obtained at 1 h post Gadobenate dimeglumine injection [10]. The MR images were retrospectively analyzed by 2 independent radiologists, who were blinded to the biopsy results.

The results obtained by both reporting methods were segregated into qualitative and LIRADS subcategories and correlated with the final histopathology diagnosis.

2.4. Image analysis

Two independent radiologists, blinded to the histological findings, evaluated all the studies, classified the lesions as per the LIRADS v2018 criteria and qualitative reporting method, in a random sequence and at different time points and the results were finalized. The overall statistical inter-observer agreement between the two radiologists was found to have a kappa value of 0.95 ± 0.05.

The imaging studies (triple phase MDCT and/or hepatocytes specific contrast enhanced MRI) of the study group (n = 302) were reviewed, reread and the lesions were described *qualitatively* as per the conventional pattern of imaging and enhancement characteristics into the following subgroups:

- Classical HCC lesions (including multifocal HCC) which showed typical hypervascular pattern followed by washout and capsule formation (Fig. 2).
- Atypical HCC (including subcategories of Hypovascular HCC

(Fig. 3), Combined Cholangio-Hepatocellular carcinoma (Figs. Fig. 44, Fig. 55), Infiltrative HCC (Fig. 6) and other such lesions which did not show characteristic pattern on imaging but were in favor of HCC [11].
- Indeterminate lesions including dysplastic nodules (Fig. 7). These lesions did not show enhancement pattern described for HCC and were difficult to classify into either benign or malignant subgroups.
- Other malignancies which were found to be difficult to distinguish from HCC on imaging; however, did not show appearance of classical HCC e.g. Neuroendocrine metastases, hypervascular metastases from adenocarcinoma (Fig. 8) [12].

The grading included LIRADS 2 -5 and LIRADS M (other malignancy) observations. The LIRADS categorization was performed, (independent of the qualitative results) using the current standardized reporting algorithm, including main and ancillary features of suspected liver lesions in patients with chronic liver disease. Both CECT and CEMRI sequences were studied in the dynamic phases as well as the supporting sequences (on MRI: Diffusion weighted sequence, T2WI, T1WI, delayed hepatobiliary phase and on CT: Non -contrast and equilibrium phase scans) (Fig. 9–12).

The contrast enhanced MDCT and MRI scan methodology for liver imaging was maintained uniformly over the study span due to standardized institutional protocols and comprised of predominantly, non-contrast scan, followed by dynamic (arterial, portal, equilibrium and delayed phases) imaging on both CT and MRI. The reviewers analyzed
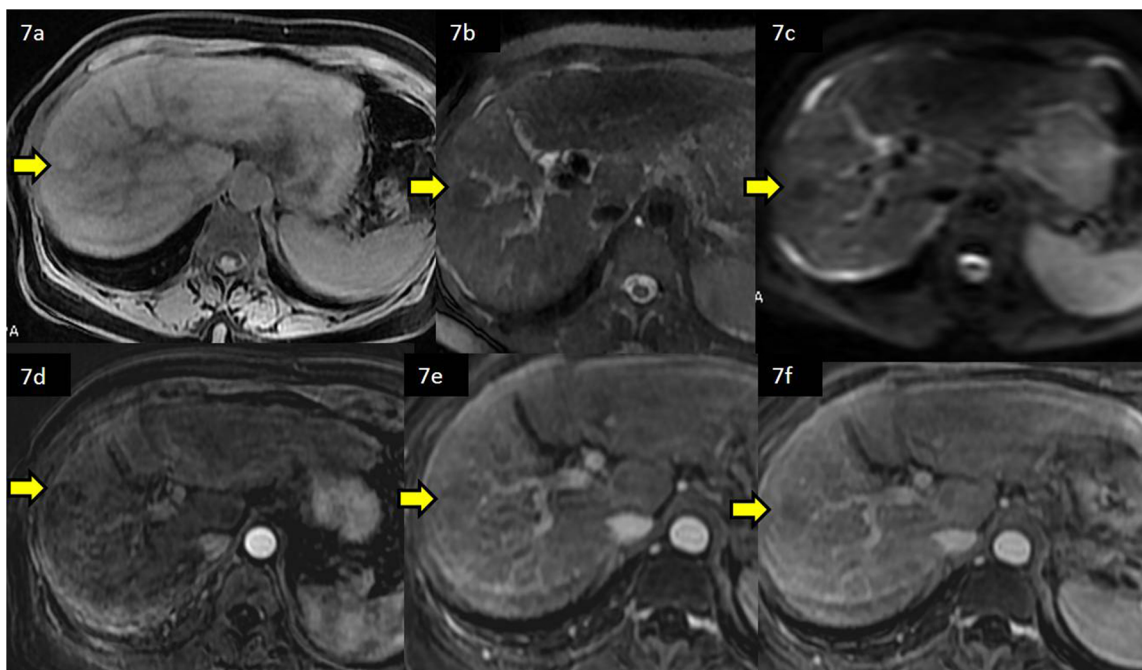
Fig. 7. Axial sections of dynamic MRI scan of a lesion in the right lobe described as 'dysplastic nodule' on qualitative imaging 7a. Non-contrast T1WI showing hyperintense 15 mm nodule (arrow) in segment VII of right lobe of liver 7b. Nodule appears T2 hypointense (yellow arrow) and is (7c) non restricting on DWI Post contrast, nodule does not show enhancement (7d) and remains non-enhancing on subsequent PVP (7e) and equilibrium (7f) phases.
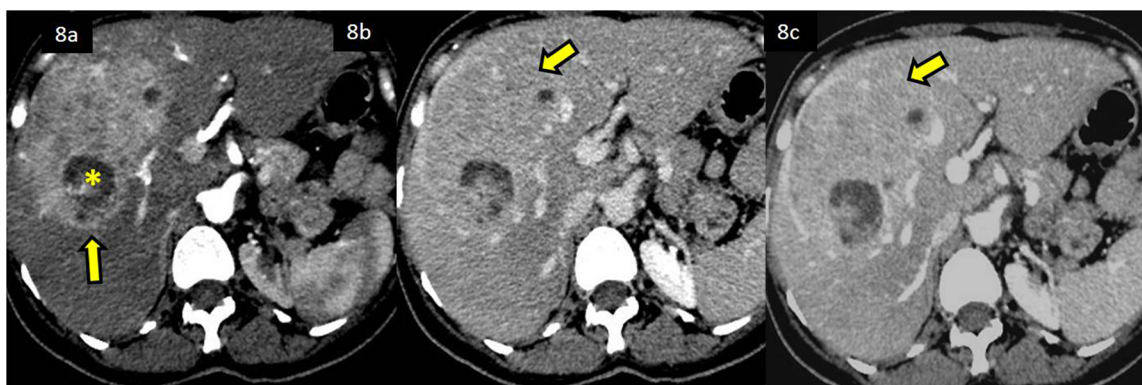
Fig. 8. Triple phase CECT scan of a lesion in the liver suggestive of HCC on qualitative imaging, diagnosed as metastatic deposit from occult neuroendocrine tumor on histopathology.

(8a) Large hypervascular mass lesion (arrow) involving segments VII and VIII of liver with internal area of fat density (*), (8b) The mass lesion shows washout on subsequent PVP and (8c) capsule formation (arrow) on equilibrium phase.

the CT and MR images (including the delayed hepatobiliary phase) for tumor size, number of lesions [single, two or three and more (≥ 3)], enhancement pattern, washout, pseudo capsule formation (as per LIRADS criteria; using both major and ancillary features).

2.5. Histopathology analysis

Histopathology diagnosis of HCC and the dysplastic lesions is based on examination of routine Hematoxylin-eosin stained tissue complemented by ancillary special histochemical stains such as reticulin and immunohistochemical antibodies such as CD34 positive capillarization of sinusoids. Unaccompanied arteries and lack of portal tracts indicate the presence of lesional tissue. Deviation from normal liver architecture with presence of sheet-like compact pattern, pseudoglandular or trabecular patterns characterise HCC. [13,14] Immunohistochemical stains Hepatocyte paraffin 1, arginase 1, Glypican-3, polyclonal CEA, CD10 combined with markers to exclude metastasis, are useful for the diagnosis of HCC and distinguishing from metastatic

adenocarcinoma and cholangiocarcinoma.

Dysplastic liver lesions are classified and characterised into low grade and high grade dysplasia and small HCC, according to the criteria laid down by the International working party in 1995 and the International consensus group for hepatocellular neoplasia in 2009 [15–17]. Difficult cases are analysed by panel of immunohistochemical markers – Glypican-3, heat shock protein 70 and glutamine synthetase [18,19].

HCC are not homogeneous and several distinct subtypes and specific variants exist. Scirrhous, sarcomatous, fibrolamellar, steatohepatitic, clear cell, oncocytic, G-CSF producing, combined hepatocellular-cholangiocarcinoma, macrotrabecular, cholangiolocellular, are more common. [20,21] Most of the variants are designated based on the presence of characteristic histomorphologic and immunohistochemical markers, in at least 50 % of the tumour

The histopathological analysis was performed by a team of two experienced liver pathologists with standard techniques and immunohistochemistry.
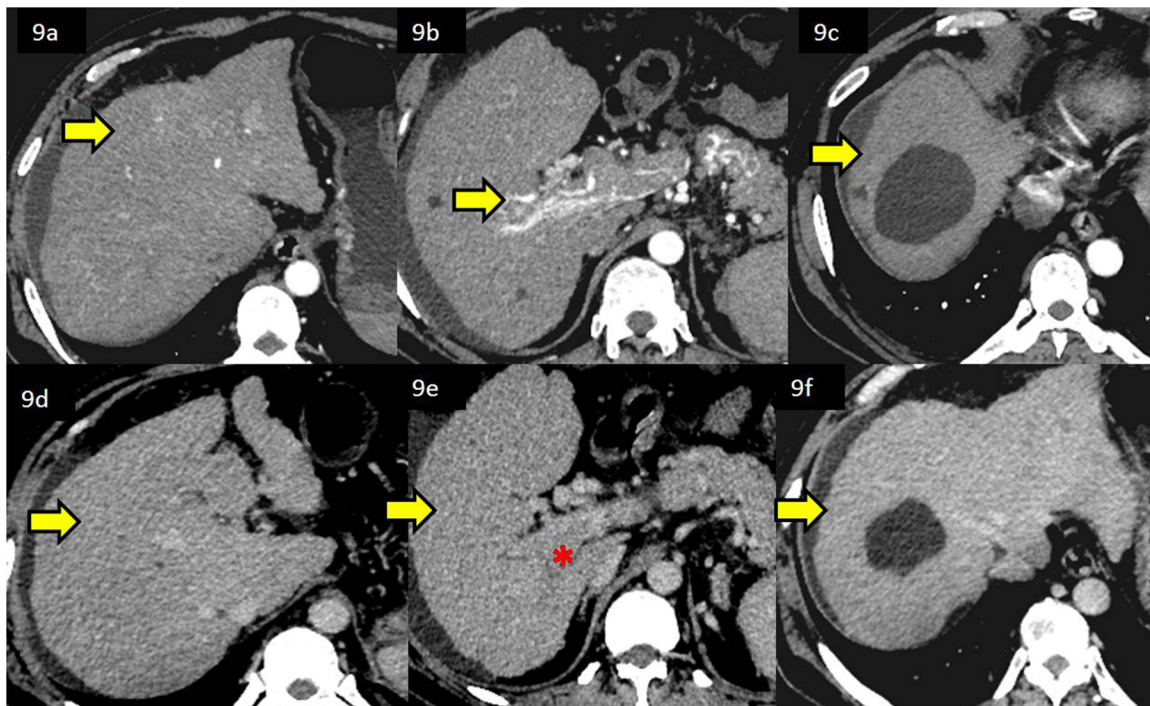
Fig. 9. Triple phase CECT scan of a LIRADs 3 observation in the liver without obvious mass seen. Biopsy showed 'cirrhosis like HCC' without a dominant mass. (9a) Ill defined areas of blush (arrow) seen in the right lobe of liver, segment VIII (9b) Tumoral thrombus in the arterial phase within the main and right portal vein (arrow) with classical (thread and streak appearance) (9c) Rounded cystic area in superior segment VIII, without obvious mass on HAP (9d, e) No obvious mass seen in segment VIII and VII on PVP (arrows) with presence of thrombus in the portal vein lumen (*) (9f) No obvious mass lesion on equilibrium phase except the cystic lesion (arrow).
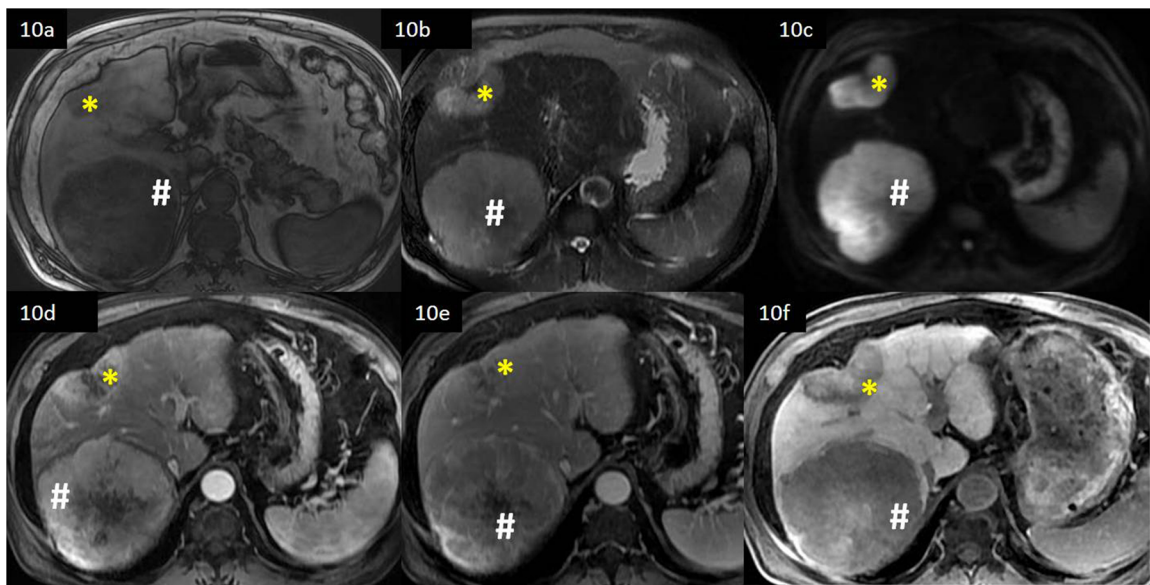

Fig. 10. Triple phase CEMR scan of LIRADS 4 observations in the liver with presence of 2 similar lesions. Biopsy showed: Lesion (#): Hepatocellular Carcinoma, Lesion (*): Cholangiocarcinoma **(Dual cancer)**.
(10a) Presence of fat within the lesion (#) with absence of fat in lesion (*) on chemical shift imaging(10b) T2W sequence showing hyperintensity of both lesions (*, #) with capsular retraction in lesion (*) (10c) Both lesions demonstrate hyperintense signal on DWI (10d) Hypervascularity with central necrosis observed in both on HAP (10e) Lesion(#) shows capsule formation with central scar, labeled as LIRADS4, lesion(*) shows persistent enhancement with central scar, labeled LIRADS 4 (atypical type) (10f) hepatobiliary phase shows partial contrast retention with washout in lesion (*) and complete washout in lesion (#).

3. Statistical analysis

Analysis was performed using SPSSv22.0 (IBM Corp. Ltd; ARMONK, NY, USA). Categorical data has been presented as frequency (n %) and continuous data expressed as mean ± standard deviation or median (IQR), as appropriate. The comparison of categorical data was done using the Chi square or Fischer exact test. The continuous data was analyzed using one-way ANOVA followed by post hoc comparison by Bonferronie method or Kruskal Wallis' test, wherever applicable. The performance characteristics of the two methods of reporting were assessed by computing the sensitivity, specificity, negative and positive predictive values as well as positive and negative LHRs, against the gold
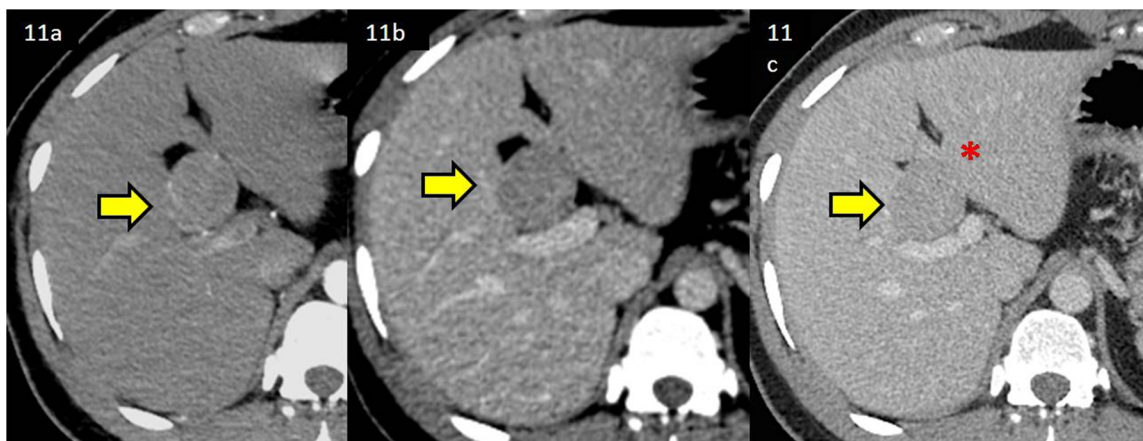
Fig. 11. Triple phase CECT scan of a LIRADS 5 observation in the liver with well defined mass. Biopsy was confirmatory for HCC.
(11a) Hypervascular rounded lesion (arrow) in segment V, IV b showing hypervascularity on Hap (11b) Subsequent washout of contrast in the lesion on PVP (arrow) (11c) Thin capsule with hypoattenuation of the lesion on equilibrium phase.
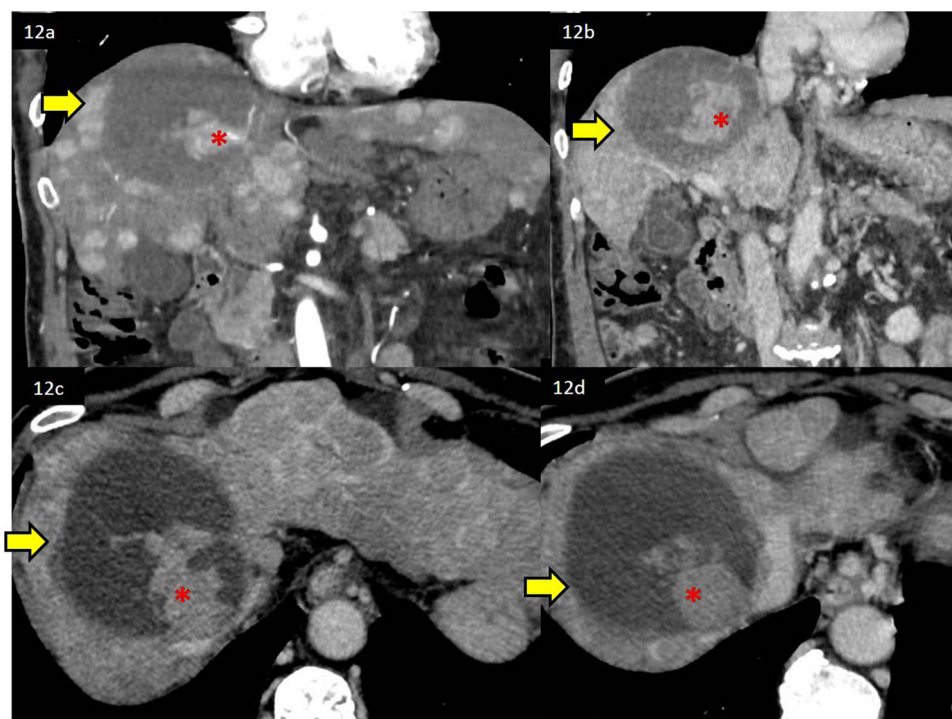
Fig. 12. Triple phase CECT scan of LIRADS M observation in the liver with multiple well defined lesions. Biopsy was confirmatory for metastases from adenocarcinoma HCC.

(12a) Multiple well defined rounded hypervascular lesions studded in both lobes of the liver on HAP with a large hypodense, necrotic lesion (arrow) in segment IV/VIII with internal hypervascular solid component (*) (12b) Multiple lesions show partial washout with central soft tissue (*) within the necrotic lesion (arrow) showing similar enhancement (12c, d) Soft tissue nodule (*) within hypoattenuating large lesion (arrow) shows washout on subsequent phases.

standard of histopathology. Kappa statistics was used to find the intra observer agreement between the two radiologists. A p value < 0.05 was considered as significant.

4. Results

4.1. Baseline characteristics and qualitative assessment

A total of 302 patients, [269 (89 %) men, mean age 57 ± 12.4 years] underwent biopsy for suspected liver lesions, over a period of ten years. These were categorized, on consensus reading, by 2 hepatobiliary radiologists (6 and 11 years' experience) as per conventional and descriptive radiological findings (qualitative imaging). Out of the total of 302 patients, indeterminate lesions including dysplastic nodules were diagnosed in 7 patients (2.3 %), atypical HCC in 68 patients (22.5 %), hypo vascular HCC in 8 patients (2.6 %), combined hepato-cholangio-carcinoma in 9 patients (3.0 %) and infiltrative HCC in 11 patients (3.6 %). Hyper vascular metastases were suspected in 9 patients (3.0 %) and

other malignancy in 11 patients (3.6 %). Classical as well as multifocal HCC were diagnosed in 102 and 76 patients respectively (33.8 %; 25.2 %). Differential diagnosis was made wherever necessary, particularly for patients not characterized as HCC (classical or atypical). The general and characteristic features of each subgroup, number of lesions, mean size and AFP levels were studied in the different subcategories and have been described in Table 1.Therapeutic strategy and follow up, were noted.

4.2. Classification as per LI-RADS lexicon

The two hepatobiliary radiologists (via consensus reading) used the LIRADS v 2018 lexicon in addition to further categorize the study group patients into primarily four categories i.e.LI-RADS 3-5 and LIRADS M, independent of the qualitative assessment. Only 1 patient with a single lesion, appearing as an area of transient attenuation difference or arterio-portal shunt was categorized as LIRADS 2. Of the total 302 patients, 42 observations (13.9 %) were deemed as LIRADS 3 category,

Table 1
General characteristics, morphology and pattern of lesions as per Qualitative imaging (descriptive conventional reporting).

Characteristics	Total lesions (n = 302)	Dysplastic Nodule (n = 7)	Atypical HCC (n = 68)	Hypo-vascular HCC (n = 8)	Combined HCC - CCa (n = 9)	Infiltrative HCC (n = 11)	Classical HCC (n = 102)	Multifocal HCC (n = 76)	Hyper-vascular mets (n = 9)	OtherMalignancy (n = 11)	p value
Sex (M/F)	269/33	6/1	61/7	7/1	9/0	8/3	93/9	68/8	8/1	8/3	0.473
Age (yr, mean ± Std.)	57.08 ± 12.43	55 ± 14.34	58.22 ± 10.22	48.62 ± 8.83	59.11 ± 15.32	57.27 ± 8.40	58.63 ± 12.23	55.26 ± 15.001	54.55 ± 12.43	57.54 ± 5.12	0.401
Lesion Size (cm) (Mean ± range)	5.19 ± 3.55	1.82 ± 1.25	4.85 ± 3.85	4.18 ± 3.94	4.18 ± 2.20	5.60 ± 3.41	5.43 ± 3.52	5.34 ± 3.30	5.18 ± 3.71	7.23 ± 4.18	0.120
Single lesion (n, %)	157 52%	6 85.7%	40 58.8%	5 62.5%	7 77.8%	5 45.5%	73 71.6%	8 10.5%	3 33.3%	10 90.9%	< 0.001
Two lesions (n, %)	30 9.9%	0	7 10.3%	3 37.5%	0	2 18.2%	13 12.7%	3 3.9%	1 11.15	1 9.1%	0.1009
3 or more Lesions (n, %)	115 38.1%	1 14.3%	21 30.9%	0	2 22.2%	4 36.4%	16 15.7%	65 85.5%	5 55.6%	0	< 0.001
Log AFP	4.01 ± 3.14	2.41 ± 1.28	3.28 ± 2.64	2.69 ± 0.94	5.26 ± 3.23	4.74 ± 3.83	4.09 ± 3.29	5.01 ± 3.33	1.71 ± 1.19	2.95 ± 3.27	0.003
Operated cases (n, %)	49 16.2%	1 14.3%	7 10.3%	1 12.5%	2 22.2%	0	31 30.3%	5 6.6%	0	2 18.2%	< 0.001
Treated with TACE (n, %)	75 24.8%	1 14.3%	14 20.6%	3 37.5%	1 11.1%	3 27.3%	30 29.4%	20 26.3%	1 11.1%	2 18.2%	0.747
Treated with RFA (n %)	41 13.6%	4 57.1%	16 23.5%	1 12.5%	0	0	16 15.7%	3 3.9%	1 11.1%	0	< 0.001
Lost To Follow up (n, %)	137 45.4	1 14.3%	31 45.6%	3 37.5%	6 66.7%	8 72.7%	25 24.5%	48 63.2%	7 77.8%	7 63.6%	< 0.001

HCC = Hepatocellular carcinoma, Cca = Cholangiocarcinoma, mets = Metastases, AFP = Alpha fetoprotein, TACE = Trans-arterial chemoembolization, RFA = Radiofrequency ablation.
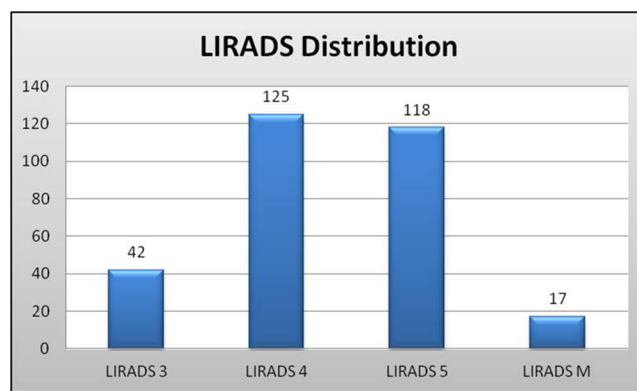
Fig. 13. Frequency of observations in each category of LIRADS depicted in graphical pattern.

125 observations (41.4 %) were classified as LIRADS 4, 17 observations (5.6 %) were classified as 'other malignancy' (LR M) and 118 patients (39.1 %) were found to be classical HCC or LIRADS 5 (Fig. 13). The detailed characteristics of these patients and classification as per LIRADS lexicon is described in Table 2. Statistical analysis was performed using the above observations. It was observed that the patients age, gender, number of lesions, tumor marker-alpha-fetoprotein (AFP) and treatment modalities were not statistically different among the above sub-groups, (p > 0.05). However, the mean lesion size was found to be significantly higher in LIRADS M category as compared to LIRADS 3 (p = 0.025). Qualitative Imaging findings demonstrated a sensitivity of 92.3 % (CI 88.53–94.91), specificity of 41.4 % (CI 25.51–59.26), PPV of 93.7 %, NPV of 36.4 %, (+ LHR) of 1.575 (CI 1.40–1.77), -LHR of 0.19(CI 0.13-0.26). Imaging correctly classified 87.4 % of the lesions diagnosed on pathology. The details of the diagnosis using conventional qualitative radiology versus the gold standard pathology diagnosis are described in Table 3. LI-RADS for lesion characterization on imaging was found to have a sensitivity of 97 %, specificity of 55.56 %, PPV of 97 % NPV of 30.3 % and diagnostic accuracy of 89.7 %. The details of imaging diagnosis using LIRADS versus the gold standard pathology diagnosis have been given in Table 4.

Comparison of all three methods i.e. LIRADS, qualitative imaging and combination of both techniques with respect to pathology as gold standard has been depicted in (Fig. 14). The kappa agreement between LIRADs and qualitative Imaging was found to be 77 ± 0 0.07 (p < 0.001). There was a significant difference between LIRADS and qualitative imaging data (p < 0.001). Ten out of 28 (35.7 %) negative HCC lesions on qualitative imaging were found to be positive on LIRADS classification. Further combination of LIRADS and qualitative imaging had sensitivity 97 %, specificity 30 %, PPV 91.9 %and NPV of 55.6 % which is same as LIRADs alone. We observed that 81 % of the total lesions categorized as LR-3; 87 % of LR-4; 94 % of LR-5 and 47 % of LR-M were found to be HCC on biopsy.

A total of 38 patients were found to have discordant diagnoses on imaging with respect to histopathology. The details of these patients are described in Table 5.

The number of lesions incorrectly diagnosed (false positive) as HCC on imaging was n = 21. Majority of these lesions belonged to LI-RADS 4 category (52.4 %). Twelve (n = 12) of these patients had primary adenocarcinoma, 4 patients had metastatic adenocarcinoma, one patient each, had gastrointestinal stromal tumor (GIST) (Fig. 15) and neuroendocrine metastasis respectively (Fig. 8). Core biopsy revealed that two patients had Fibrolamellar carcinoma (Figs. Fig. 1616, Fig. 1717) and one patient was diagnosed with Telangiectatic adenoma (Fig. 18). The above three patients had background liver parenchymal disease with normal AFP values.

Amongst the false positive cases, majority of the patients had multiple lesions (n = 14, 67 %). No differential diagnosis was provided in

Table 2

General characteristics of liver lesions as per: Liver imaging reporting and data system version 2018 (LI-RADSv2018) lexicon.

Characteristics	Total lesions (n = 302)	LIRADS 3 (n = 42)	LIRADS 4 (n = 125)	LIRADS 5 (n = 118)	LIRADS M (n = 17)	p value
Sex (M/F)	269/33	38/4	111/14	107/11	13/4	0.335
Age (yrs, mean ± Std.)	57.08 ± 12.43	57.28 ± 11.16	58.34 ± 11.56	56 ± 14.09	54.70 ± 8.66	0.423
Lesion Size (cm) (Mean ± range)	5.19 ± 3.55	4.07 ± 3.33	5.39 ± 3.61	5.11 ± 3.40	7.05 ± 3.88	0.025* (LR-M vs. LR-3)
Single lesion (n, %)	157 52%	19 45.2%	68 54.4%	58 49.2%	12 70.6%	0.28
Two lesions (n, %)	30 9.9%	6 14.3%	15 12.0%	8 6.8%	1 5.9%	0.38
Three or more lesions (n, %)	115 38.1%	17 40.5%	42 33.6%	52 44.1%	4 23.5%	0.21
Log AFP	4.01 ± 3.14	3.41 ± 2.17	4.18 ± 3.26	4.24 ± 3.30	2.35 ± 2.84	0.064
AFP median (IQR values)	15.18 (5.96 – 207.97)	12.14 (7.58- 93.50)	15.38 (6.22- 288.98)	17.80 (6.27 – 235.59)	3.31 (2.38-26.51)	0.019* (LR-M vs. all others)
Operated cases (n, %)	49 16.2%	3 7.1%	14 11.2%	30 25.4%	2 11.8%	0.005* (LR-M vs. LR-4,5), (LR-3 vs. LR-4,5)
Treated with TACE (n, %)	75 24.8%	8 19%	28 22.4%	36 30.5%	3 17.6%	0.301
Treated with RFA (n, %)	41 13.6%	11 26.2%	17 13.6%	13 11%	0	0.02* (LR-M vs. all others)
Lost To Followup (n, %)	137 45.4%	20 47.6%	66 52.8%	39 33.1%	12 70.6%	0.002* (LR-M vs. LR-4,5)

HCC = Hepatocellular carcinoma, AFP = Alpha fetoprotein, TACE = Trans-arterial chemoembolization, RFA = Radiofrequency ablation, LIRADS 3 = Indeterminate lesions, LIRADS 4 = Likely or probably HCC, LIRADS 5 = Definitely HCC, LIRADS M = other malignancy or metastases besides HCC, * = significant.

Table 3

Qualitative Imaging Versus Histopathology diagnosis.

Pathology diagnosis	Atypical HCC (n = 68)	Hypo-vascular HCC (n = 8)	Multifocal HCC (n = 76)	Combined HCC -CCa (n = 9)	Infiltrative HCC (n = 11)	DysplasticNodule (n = 7)	Hyper-vascular mets (n = 9)	Classical HCC (n = 102)	Other Malignancy (n = 11)
HCC (n) % p value = < 0.001	59 86.8%	5 62.5%	65 85.5%	7 77.8%	9 81.8%	6 85.7%	3 33.3%	100 98%	8 72.7%
AdenoCa, Cholangio-carcinoma	3 4.4%	2 25%	6 7.9%	2 22.2%	2 18.2%	0	0	2 2%	1 9.1%
Metastatic Adeno Carcinoma	1 1.5%	0	3 3.9%	0	0	0	1 11.1%	0	1 9.1%
Neuroendocrine metastases	0	0	1 1.3%	0	0	0	2 22.2%	0	0
Combined HCC-CholangioCa	1 1.5%	1 12.5%	1 1.3%	0	0	0	0	0	0
Other malignancy lymphoma/ mesenchymal	1 1.5%	0	0	0	0	0	3 33.3%	0	1 9.1%
No malignancy	3 4.4%	0	0	0	0	1 14.3%	0	0	0

HCC = Hepatocellular carcinoma, AFP = Alpha fetoprotein, TACE = Trans-arterial chemoembolization, RFA = Radiofrequency ablation, LIRADS 3 = Indeterminate lesions, LIRADS4 = Likely or probably HCC, LIRADS5 = Definitely HCC, LIRADSM (LR M) = other malignancy or metastases.

this subset, implying that imaging diagnosis was reasonably confident about these being HCC. The mean AFP in this group was raised to 927 ng/ml or mean log AFP was raised t 2.58 ± 2.04 ng/ml. A total of 15 (71 %) patients had obvious cirrhosis, whereas the rest had features of liver parenchymal disease without florid end stage changes in the liver.

Imaging missed HCC lesions (false negative) in 17 patients which were later diagnosed on biopsy. Analysis of these false negative cases revealed that majority (n = 14, 82.4 %) were solitary lesions. The mean log AFP of 2.26 ± 1.29 ng/ml (range 0–8.5 ng/ml) was normal. Interestingly, a differential diagnosis of HCC was given in 53 % of these patients. The next closest differential diagnosis described on imaging was 'target like metastases' (approximately 18 % patients). An imaging diagnosis of dysplastic nodule was made in 6 patients (Fig. 7). Two patients were diagnosed as hilar cholangiocarcinoma and hypervascular metastases were reported in three patients. Two lesions were reported as cholangiocarcinoma (Fig. 19) and hepatic adenoma each, one lesion was incorrectly diagnosed as inflammatory visceral larva migrans

(Fig. 20).

5. Discussion

The recently updated guidelines, from the American Association for the Study of Liver Diseases (AASLD) in 2018, propose that HCC can be diagnosed in a non-invasive manner with the classical enhancement pattern of hypervascularity followed by washout on dynamic liver imaging by CT or MRI. This is recommended for lesions measuring ≥ 1 cm in size and is applicable to patient populations suffering from HBV-HCV induced chronic liver disease and cirrhosis of variable etiology [22,23].

The American college of radiology has integrated the LIRADS systems along with the AASLD practice guidelines and due to the widespread uniformity of the algorithm; it is being used extensively in North America, as well as, other parts of the world for HCC reporting practices [24]. It has been reported and discussed in literature that HCC is one of

Table 4
Imaging classification as per LIRADS lexicon versus Pathology diagnosis.

Pathology Diagnosis	LIRADS 3 (42)	LIRADS 4 (125)	LIRADS 5 (118)	LIRADS M (17)
Primary Cholangio Carcinoma	3 7.1%	8 6.4%	6 5.1%	1 5.9%
Metastatic Adeno Carcinoma	0	4 3.2%	0	2 11.8%
Neuroendocrine metastases	0	0	1 0.8%	2 11.8%
Combined HCC-CCa	0	3 2.4%	0	0
Other malignancies lymphoma/ mesenchymal tumors	0	1 0.8%	0	4 23.5%
No malignancy	5 11.9%	0	0	0
Definite HCC **	34 81%	109 87.2%	111 94.1%	8 47.1%

** p < 0.001, LIRAD M had significantly lower value as compared to LIRAD-3,4and LIRAD 5 values.

the few malignancies where imaging studies play a key role in diagnosis and many times in management using imaging guided ablation and chemotherapy. An early diagnosis of liver lesions suspected to be HCC or its variants can impact the patient's survival and chance of radical therapy or surgery [25,26]. In our study, we assessed the spectrum of HCC and the influence of potential confounding factors on image-based diagnosis of HCC in patients with cirrhosis. Detailed analysis was performed to observe the factors, due to which, imaging was unable to provide a definitive diagnosis of HCC with histopathology as a gold standard for the confirmatory diagnosis.

Rastogi A. has quoted that almost 10–15 % of all patients with equivocal results on imaging have been subjected to biopsy irrespective of the lesion size, more so, in cases of well differentiated HCC's. [27,28] Our study data corresponds to this analysis. The number of patients (n = 302) who underwent histopathology evaluation over a span of 10 years was equivalent to 10 % of the total (n = 2916) number of patients who demonstrated classical enhancement pattern of HCC (not requiring further biopsy) during the same time period. This figure also provides us an approximate percentage of patients in daily clinical practice who are likely to benefit from an improved imaging based diagnostic protocol.

A higher proportion of men (89 %) was observed in both qualitative and LIRADS groups, although gender did not statistically (p > 0.005) influence diagnostic accuracy amongst our study group. This observation was made previously by Lai et al. who demonstrated, that, males not only have a higher predisposition to develop HCC but also have a poorer prognosis compared to females during the post-operative period,

Table 5
Discordant cases on imaging with respect to Histopathology.

Characteristics (n)	False negative cases (Missed on imaging) which were HCC on pathology (17)	False positive cases (Misdiagnosed as HCC on Imaging) which were non HCC on pathology (21)	p value
Age in yrs (mean ± Std.)	57.82 ± 10.33	59.475 ± 9.19	0.605
Lesion Size (Mean) (in cms)	4.12 ± 4.09	4.38 ± 4.40	0.852
Number of lesions (single) (n, %)	14 82.4%	5 23.8%	< 0.001
Number of lesions (2 lesions)	1 5.9%	2 9.5%	0.678
Number of Lesions (≥3)	2 11.8%	14 66.7%	< 0.001
Log AFP	2.26 ± 1.29	2.58 ± 2.04	0.577
Operated (n, %)	3 17.6%	1 4.8%	0.198
Treated with TACE(n, %)	2 11.8%	1 4.8%	0.426
Treated with RFA(n, %)	5 29.4%	1 4.8%	0.0382
Lost To Follow up(n, %)	7 41.2	18 85.7%	0.004
D/D- target like mets (n, %)	3 17.6%	2 9.5%	0.461
D/D – dysplastic nodule(n, %)	0	0	-
D/D – hypervascular mets (n, %)	1 5.9%	3 14.3%	0.401
D/D hypovascular HCC (n, %)	0	1 4.8%	0.361
D/D other malignancy (n, %)	0	0	-
D/D HCC-Cca (n, %)	0	1 4.8%	0.361
D/D less likely HCC(n, %)	9 52.9%	0	< 0.001
No D/D (n, %)	4 23.5%	14 66.7%	0.008
LIRADS 3 (n, %)	9 52.9%	4 19%	0.028
LIRADS 4 (n, %)	3 17.6%	11 52.4%	0.027
LIRADS 5(n, %)	2 11.8%	6 28.6%	0.206
LIRADS M(n, %)	3 17.6%	0	0.044
Cirrhotic (n, %)	7 41.2%	15 71.4%	0.060
Liver parenchymal disease (n, %)	10 58.8%	6 28.6%	0.060

Comparison of all reporting systems w.r.t. Histopathology

Legend: Qualitative Imaging; lirads; Qualitative imaging +LIRADS

Values shown: Sensitivity: 97, 92.31, 91.9; Specificity: 55.56, 41.38, 30; PPV: 97.03, 93.68, 91.9; NPV: 55.6, 36.36, 30.3; DA: 89.74, 89.7, 87.42
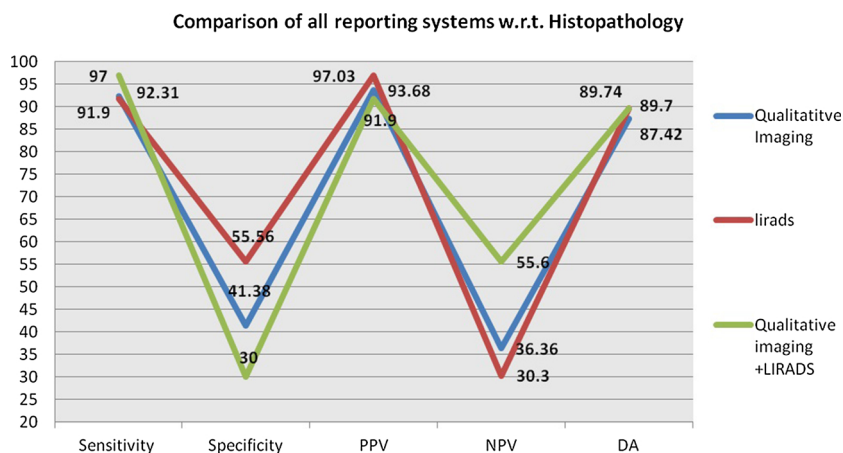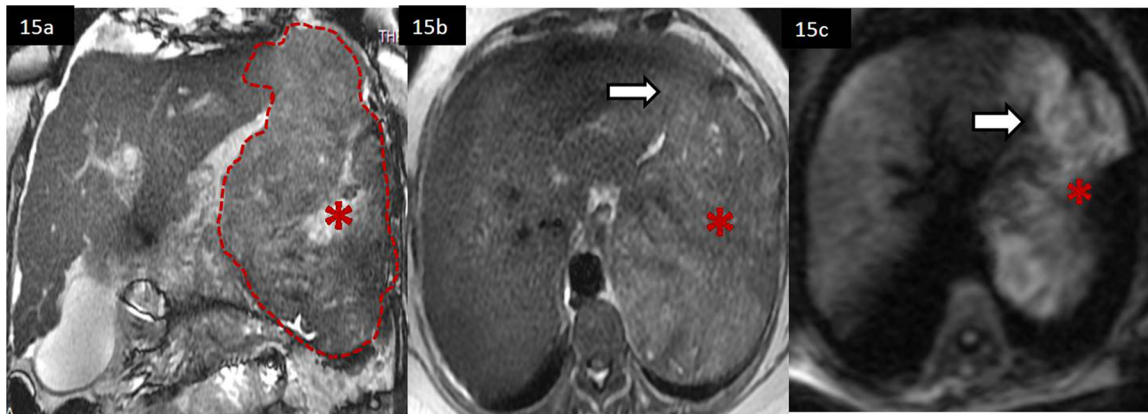
Fig. 14. Comparison of LIRADS method, qualitative imaging method and their combination with respect to pathology as gold standard.

Fig. 15. MRI upper abdomen of a large left hypochondrial mass lesion diagnosed on imaging as 'Gastrointestinal tumor of the stomach' (Discordant diagnosis on Imaging) Biopsy confirmed the lesion as exophytic HCC.
(15a) Coronal FIESTA sequence depicting a large soft tissue mass lesion (dotted lines) with central scar (*) appearing mildly hyperintense compared to the liver parenchyma, compressing the stomach and occupying the gastric region(15b) Axial T2 weighted sequence depicting the mass lesion appearing hyperintense to the liver (arrow) (15c) Mass appearing hyperintense on DWI sequence (*).
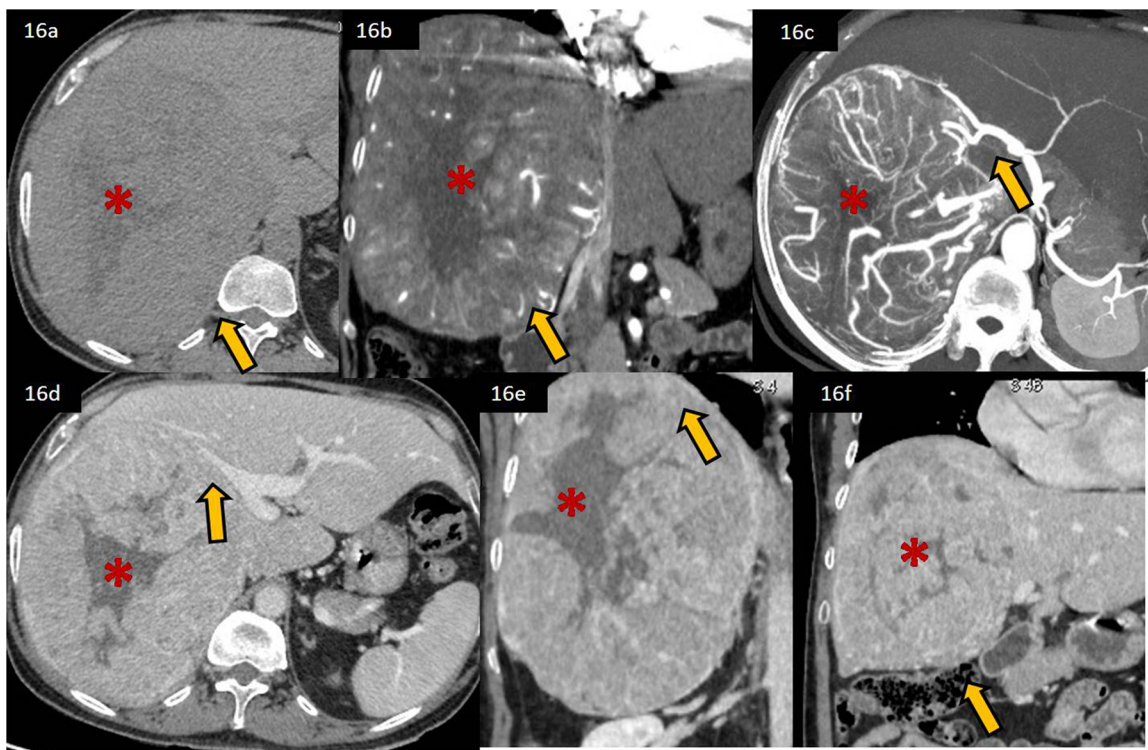
Fig. 16. Triple phase CECT of upper abdomen, diagnosed on imaging as HCC (Discordant diagnosis on Imaging) Post operative histopathology confirmed the lesion as Fibrolamellar carcinoma.
(16a) large soft tissue mass lesion with central scar (*) appearing mildly hypodense compared to the liver parenchyma (16b) Mass shows intense arterial hypervascularity (arrow) (16c) Maximum intensity projection showing vascular supply of the tumor from the right hepatic artery, sparing the centre of the lesion (*) (16d) Tumor is seen to splay and compress the right portal vein (arrow) (16e) Central scar remains hypodense, necrotic (*) with washout of the lesion in periphery and splaying of the portal vein (arrow) (16f) Mass is hypodense on equilibrium phase (arrow) occupying almost the entire right lobe of liver.

disease progression and overall survival [29].

Qualitative imaging observations, showed lowest mean age: (48.6 ± 8.8 years) in patients with hypovascular HCC versus the highest mean age of 59.1 ± 15.3 yrs. (p value > 0.005) in patients with combined Hepato-cholangiocarcinoma. Hypovascular HCC is constituted by a cohort of nodules which are detected early or represent well differentiated form of HCC; often seen in younger patients. [30] Similar, hypovascular pattern, is seen in 'sarcomatous variant' of HCC, which also affects a relatively younger age group (35–55 yrs) [31–33]. No statistical difference in the age group was observed, amongst either

qualitative (p = 0.401) or LIRADS (p = 0.423) sub groups within the study. We made an interesting observation that the age group of patients with atypical lesions was lower than the mean age described in various studies for classical HCC (50–70 years) [34,35] It may hence, be kept in mind that detection of atypical HCC tumors becomes even more important for patients who belong to the active middle age group.

Lesion size was observed to be an insignificant factor for diagnostic accuracy on comparing all subgroups of biopsied patients in both qualitative and LIRADS system of reporting in our study. Paisant et al studied the effect of extracellular (ECA) and hepatocyte specific (HPB)
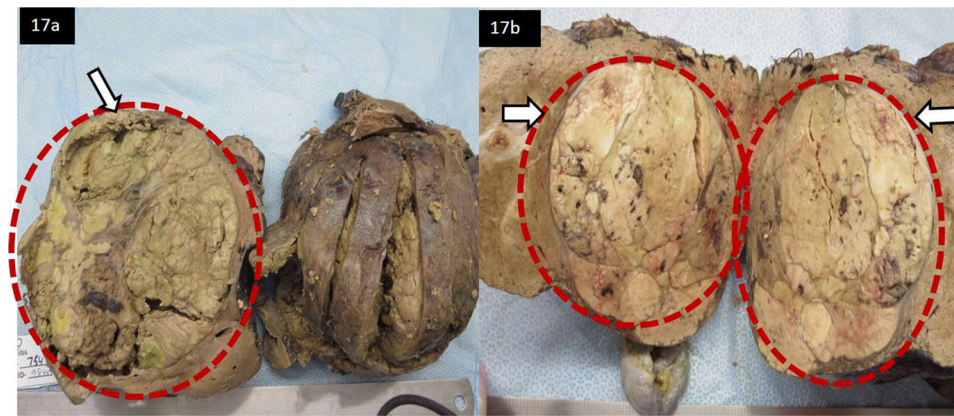
Fig. 17. Gross cut section of the tumor (arrow) well encapsulated (dotted circle) within the right lobe of liver.
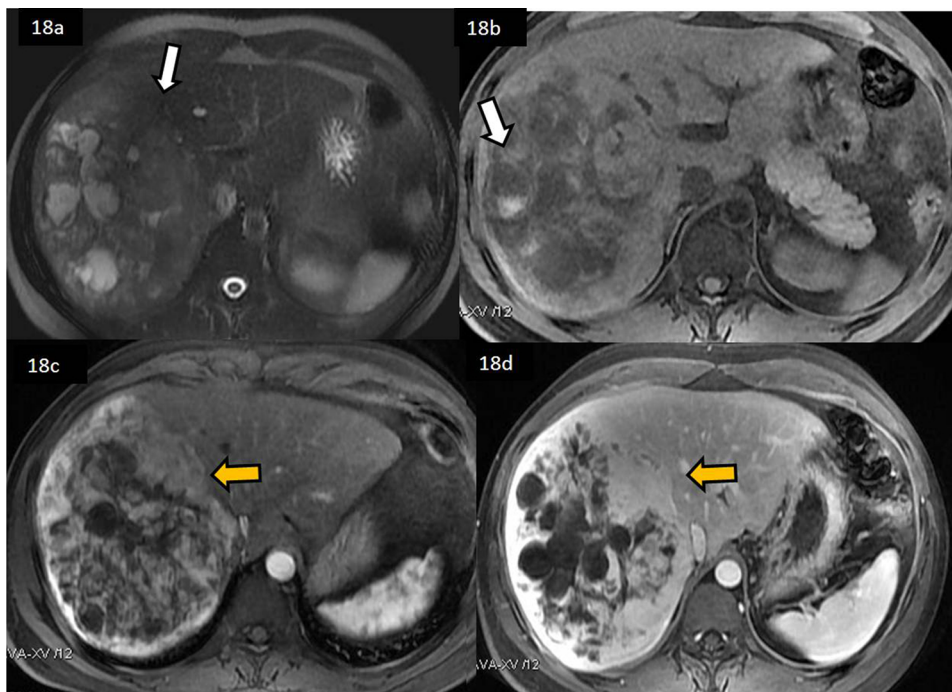

Fig. 18. Dynamic CEMRI of the liver in a 35 yr male patient, positive for hepatitis B, diagnosed as HCC on imaging (Discordant diagnosis on Imaging). Biopsy confirmed the tumor as Telangiectatic adenoma.

(18a) Axial T2 weighted sequence depicting the heterogeneous, hyperintense mass lesion with multiple necrotic areas within (arrow) occupying the right lobe of liver (18b) T1 weighted sequence shows areas of hyperintensity with fluid-fluid layering within the necrotic spaces suggestive of hemorrhage/debris (arrow) (18c) Post contrast mass shows diffuse areas of hypervascularity (arrow) with (18d) diffuse peripheral enhancement and central non enhancing areas within.

MR contrast agents for diagnostic efficacy of suspected HCC nodules and demonstrated that there was no significant difference in diagnosis using either agent especially in < 2 cms lesions. [36] Interestingly, Paisant et al. showed that, diagnostic specificity was better for ECA compared to HPB agents for lesions > 3 cms.

We made an unusual observation in our study; that all lesions which were biopsied were > 3 cms with an average size of 5.2 ± 3.6 cm, smallest mean size of 1.8 ± 1.3 cm (in dysplastic nodule group) and largest mean size of 7.2 ± 4.2 cm (in 'other malignancy' group). This finding was contrary to the notion that the undiagnosed, atypical or indeterminate lesions on imaging are usually $\leq 1-2$ cm. Most of the current guidelines advocate the application of radiological diagnostic algorithms for lesions > 1 cm and use of more than one modality or trouble shooting methods for better diagnostic accuracy for lesions $1-2$ cm in size [37]. Similarly, using LI-RADS classification, the group of LR 3, observations had a smaller mean size of 4.1 ± 3.3 cm as compared to the group of LR-M observations which had a significantly larger mean size of 7.1 ± 3.9 cm (p = 0.025). Shin et.al have described most of the patients in their study showing mean size of < 3 cm demonstrating atypical enhancement of HCC [38]. In a study by Kim. I et.al, the mean size of HCC's with classic enhancement pattern was significantly larger than atypical enhancing HCC's. They also observed a statistically significant bigger fraction of classically enhancing HCC's between 2 cm and 3 cm in diameter [39]. Similar results have been published by Hytiroglou P and Monzawa.S et al. [40,41].

In our study, 'atypical HCC' showed a mean size of 4.9 ± 3.9 cm, which was almost similar to the classical HCC group (mean size of 5.4 ± 3.5 cm) (p value > 0.05) pointing to the fact that lesion size was not a confounding factor for our cohort. Dysplastic nodule showed the smallest mean size of 1.8 ± 1.3 cm. This is an interesting observation and highlights the fact that evolution of HCC is not just a gradual development of the enhancement pattern but also the gradual but definite increase in nodule size during the course of its evolution. The only group where lesions were larger than HCC was the non-HCC tumors or the LRM. There was significant difference (p = 0.025) between size of LRM (7.1 ± 3.9 cm) and LR3 (indeterminate group) observations which were smaller (4.1 ± 3.3 cm). This may be kept in mind in case of a diagnostic dilemma where it may be prudent to call a larger lesion: non-HCC tumor, especially if it is of indeterminate imaging characteristics.

Expected diagnostic dilemma while reporting HCC nodules is usually for smaller lesions ($1-2$ cms) (as per guidelines by AASLD/EASL). It would be worthy to emphasize; the role of enhancement
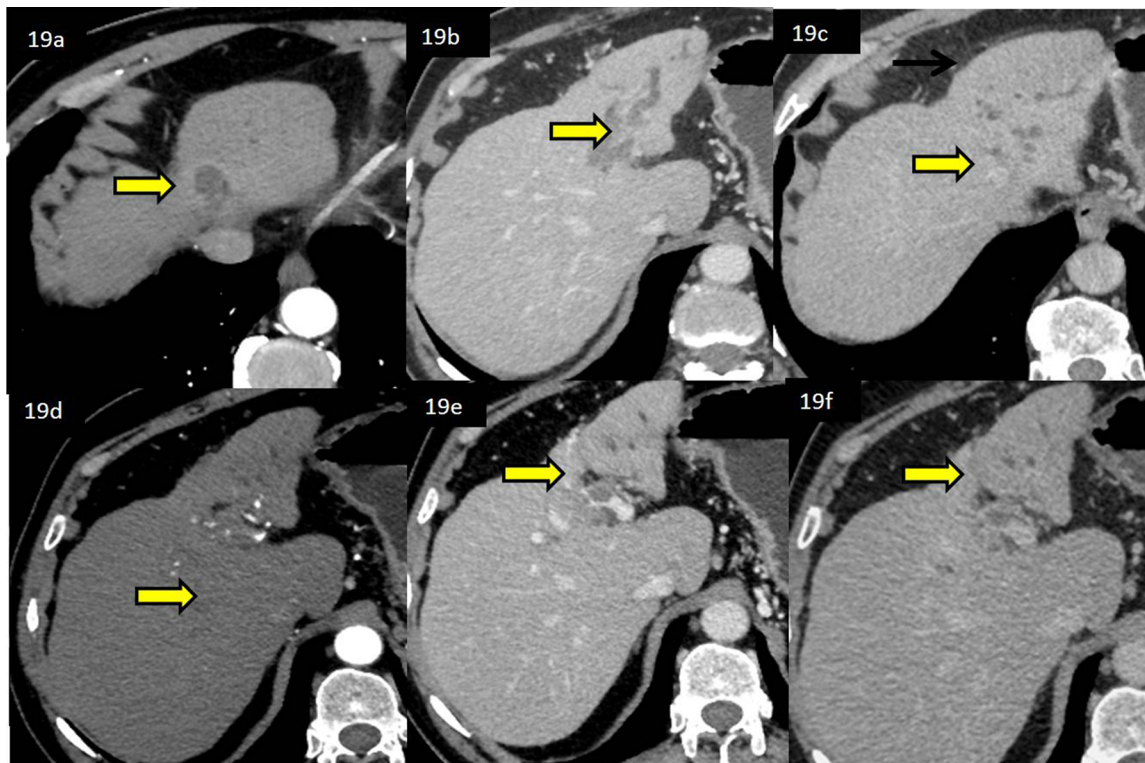
Fig. 19. CECT triple phase study of the liver diagnosed as Cholangiocarcinoma (discordant diagnosis on Imaging) Biopsy confirmed the lesion as Combined Hepatocellular Carcinoma and Intraductal Cholangiocarcinoma **(**Predominant component of Multicentric Hepatocellular Carcinoma.
(19a) mildly enhancing focal area in segment II (arrow) on HAP in left lobe of liver (19b.) Left duct mural thickening (bold arrow) on PVP with dilated ducts (arrow) (19c) Delayed phase shows isodense tumor (arrow) with atrophic left lobe (19 d) No significant enhancement of caudal portion of tumor (arrow) on HAP (19e) Hypodense soft tissue with extension (arrow) & thrombus in Left PV (*) (19f) Delayed phase showing tumor extension into bile duct (arrow) and Left PV (*).

pattern of suspected hepatic lesions rather than their size. This is especially important when the lesions in question are indeterminate/atypical or LR3 observations. We hypothesize that existing international recommendations are most useful for the 'garden' variety of HCC nodules and different guidelines may be formulated in the future for indeterminate lesions

The total number of HCC lesions in the liver are an important survival and prognostication factor since tumor burden determines the therapy which may be accorded to these patients. This has been amply documented in literature with lesion diameter cut off at $2-3$ cms permitting a good prognosis via surgery and medical management [42].

Majority of sub-groups in the qualitative category in our study had 1–2 lesions except the hypervascular metastases group where most (55.6 %) of the patients showed ≥ 3 lesions. In the LIRADS group, *1–2* lesions formed majority of observations (62 %) (p = 0.28), versus multiple (≥ 3) nodules (38 %). 'Two' lesions were seen in the least number (10 %) of observations. Most of the indeterminate and unconfirmed nodules via qualitative or LI RADS classification were solitary lesions. Majority (70.6 %) of LIRADS M lesions which underwent biopsy were also solitary lesions. This indicates a lower diagnostic probability for atypical solitary lesions because of difficulty in categorization compared to the 'classical variety'. These included 'non-HCC 'and 'other malignancy' groups in the qualitative groups too. e.g. solitary metastases from NET were misdiagnosed as HCC.

Amongst all discordant lesions, 83 % of all missed HCC's were solitary (p < 0.001). On the other hand, 67 % amongst the group of (> 3) multiple discordant lesions were diagnosed as metastases or non-HCC on imaging and were also corroborated on histopathology as non-HCC lesions (p < 0.001). (Table 5)

Lesion number plays an important role in the diagnostic bias of the radiologist while reading examinations, especially in niche areas of; atypical or indeterminate nodules in the diseased liver. This is one of

the most important confounding factors for analysis of lesions in the cirrhotic liver.

AFP which is a serum biomarker of HCC has been recommended by Canadian and Japanese guidelines during late stage or definitive tumor diagnosis as well as to assess the efficacy of treatment. [43] International guidelines by AASLD, EASL ESMO or Australian groups do not recommend AFP for standard diagnosis of HCC and almost completely rely on imaging modalities. Mia et al. demonstrated that, not only did AFP have a sensitivity of 63.3 % and specificity of 80.8 % as a tumor marker for diagnosis of HCC; it was able to discriminate between grades of tumor differentiation [44]. As a diagnostic test, when added to ultrasound assessment, AFP has been shown to have good diagnostic sensitivity at > 20 ng/ml and adequate specificity at > 200 ng/ml [45].

AFP values showed a statistically significant ((p = 0.003).) difference among various subcategories in both qualitative and LIRADS groups in our study. A rising trend of AFP was noted in patients from dysplastic nodules (minimum AFP levels) to infiltrative HCC (maximum values) in the garden subtypes of HCC. (Table 1,2) The subgroup of 'hypervascular metastases' on qualitative imaging had the smallest mean log AFP of 1.71 ± 1.19 ng/ml. The highest Log AFP was observed in the combined hepato-cholangiocarcinoma group followed by multifocal HCC. The AFP values in the LI RADS subgroups showed an ascending pattern (p > 0.005) from LR3 to LR 5 observations while non-HCC (LRM) category had the lowest median AFP of 3.31 (IQR 2.38–26.51) ng/ml (p = 0.019). Atypical category of HCC showed a mid- range of values compared to classic HCC. Our study results, reemphasize the importance of the supportive role of AFP values in the diagnosis of primary liver cancer, especially the indeterminate lesions, regardless of the method used for analysis. Both methods in our study showed a distinctive and predictable pattern in the variation of AFP levels with adequate support from histopathology as per the tumor
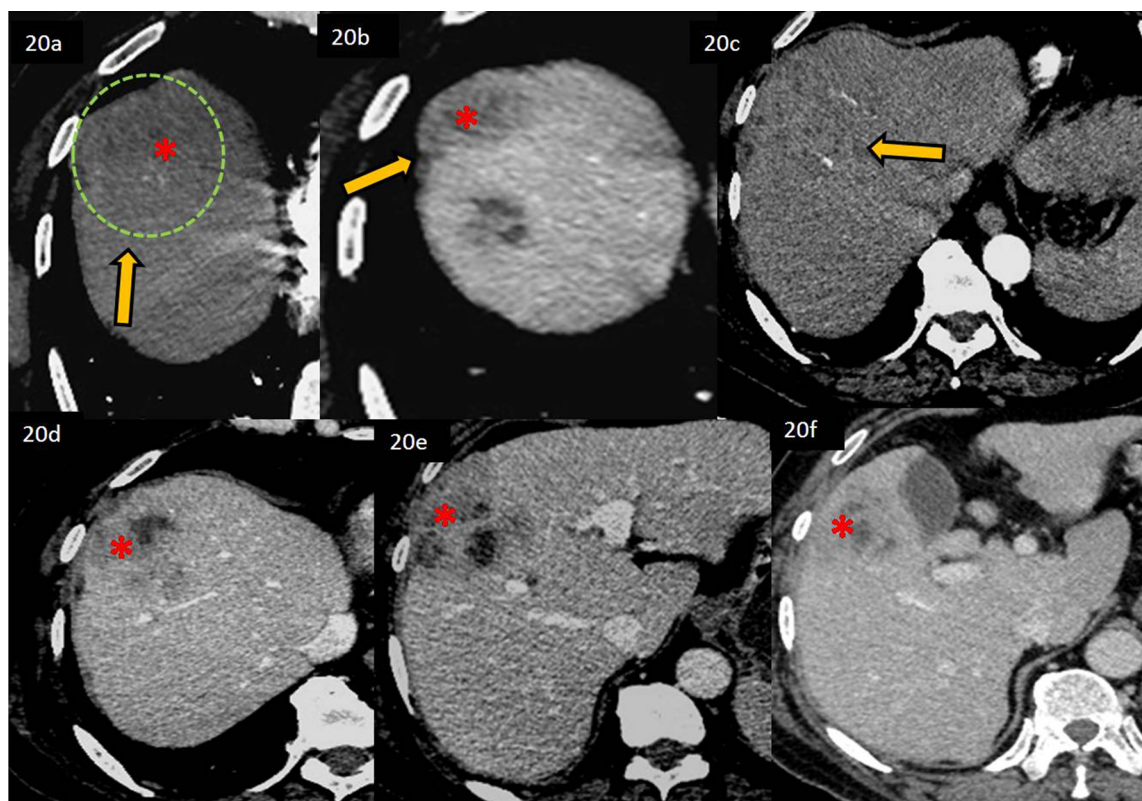
Fig. 20. CECT triple phase study of the liver, imaging diagnosis of inflammatory Pseudo-tumor/Visceral Larva Migrans (Discordant diagnosis). Biopsy confirmed lesion as HCC.

(20a) Ill defined lesion (*) in segment VIII (dotted circle) without obvious vascularity on HAP (20b) Lesion shows partial exophytic component (arrow) with central necrosis (*) (20c) No hypervascularity is seen within the lesion (arrow) (20d) lesion shows partial persistent enhancement on PVP (*) (20e) Locules with septations (*) are seen within the mass lesion (20f) Caudal extent of the tumor is present with soft tissue peripheral enhancement.

type. In case of early or small tumors, biomarkers are not adequately sensitive for diagnostic accuracy [46].

We recommend the use of AFP levels in case of indeterminate lesions in the liver as a good supplementary tool for categorization ranging from benign to malignant.

Majority (87 %) of the indeterminate lesions which were biopsied in the qualitative reporting group were correctly classified. In addition, it was observed that 'definite HCC' was the major diagnosis in all categories except 'hypervascular metastases'. Cholangiocarcinoma was the next most common diagnosis across the board, followed by 'metastases from adenocarcinoma', NET and other primary malignancies. It was observed that false positive diagnosis of HCC was made only in cases of dysplastic nodules and atypical HCC (n = 3).

Amongst the 'dysplastic nodules' category, only 1 patient was found to have absent dysplasia on biopsy. Histopathology remains the gold standard for diagnosis of dysplasia. [27] Our study has demonstrated that imaging has the potential to become a robust modality for diagnosis and possible replacement of biopsy in diagnosis of dysplastic nodules in the liver. It can also be safely claimed, as per our results, that imaging alone is able to predict more than 86 % of the 'atypical' variety of liver lesions in patients with underlying liver disease.

In addition, we can also presume that in an underlying cirrhotic or diseased liver an indeterminate lesion is 'malignant unless proven 'otherwise. This presumption in cases of indeterminate nodules would act as a red herring for the purpose of 'triaging' those who deserve priority management.

Of the LIRADS observations which underwent biopsy; > 80 % of LIRADS 3-4 and almost half of the LRM lesions were 'HCC' on pathology. This essentially means that indeterminate or atypical lesions which are LIRADS 3 observations may be considered as LIRADS 4 when contemplating immediate management strategy. Except for LIRADS 3

observations, no other category showed benign lesions on histopathology. This was an important finding with respect to decision making and formulation of a timeline for managing these patients.

We accurately predicted most of the LR5 observations (correctly classified 94 %) as 'definite HCC'. About 81 % of indeterminate cases (LR3; n = 42) and 87 % of probable HCC (LR4) observations eventually turned out to be HCC on histopathology. Frequency of observations in each category has been depicted in the graph shown in (Fig. 13). Maximum observations were categorized as LR 4 (n = 125) amongst the study population. Most clinicians would consider expediting the management of LR 4 while conferring them a 'virtual LR5′ status, from a practical standpoint.

A large proportion (81 %) of LR3 lesions were HCC on final histopathology. Hence, from a management point of view, LR3 also deserves to be fast tracked to early biopsy and confirmation of histological diagnosis so definitive treatment for HCC may be provided at the earliest.

LR-M represents malignant observations encompassing non-HCC tumors. [47] In this study histopathology results corroborated with HCC in almost half (47 %) of LRM lesions (p < 0.001). There has been an improvement in diagnostic accuracy for LRM observations after the revision of imaging features in LIRADS v2017n and v'18, however, further analysis and studies are required to formulate the best way to diagnose non-HCC tumors in cirrhotic patients with better specificity.

Ten out of 28 (35.7 %) negative HCC lesions on qualitative imaging were found to be positive on LIRADS classification. This goes in favor of the latter which showed a kappa of 77 (p < 0.001) with the former. It may also be inferred that LIRADS can be a better guide in segregation of observations for the purpose of biopsy when faced with tricky diagnostic dilemmas. A combination of both classifications was found to be similar to 'LIRADS only' in the overall diagnostic accuracy [48].

Approximately 12 % of the total lesions (38/302) in the entire

population were discordant on imaging versus pathology. (Table 5) More than half (53 %) the HCC lesions which were missed on imaging, belonged to LR 3 category. Most (82.4 %) of them were single lesions with near normal mean AFP (23.85 ng/ml); whereas the false positive lesions (67 %) were mostly multiple and had raised mean AFP levels

Number of lesions was found to be a significant predictor (p < 0.001) for false positive results on imaging. More than 3 lesions, seemed to have a higher probability of misdiagnosis and of being called multifocal HCC, especially due to mild-moderate elevation of AFP in these patients. Similarly, solitary lesions were falsely labelled as non-HCC lesions (p < 0.001). Lesion size, AFP, underlying liver disease versus full blown cirrhosis, differential diagnosis, qualitative versus LIRADS classification and management did not bear any significance between the discordant lesions on radiology versus pathology. Amongst the discordant cases, more than half (n = 9/17, 53 %) of 'missed HCCs' on imaging were called 'less likely to be HCC' as differential diagnosis and were categorized as LIRADS 3 (indeterminate nodules). We can reasonably affirm that the combined use of LIRADS and qualitative imaging in diagnosis of atypical HCC's is a reliable diagnostic tool, vis a vis biopsy which may be reserved for perplexing lesions.

6. Conclusion

It was observed that the LI-RADS v2018 lexicon along with qualitative imaging as a combination technique added extra value in interpretation of atypical, suspicious HCC or indeterminate lesions on dynamic CT and MRI compared to either qualitative conventional imaging or LIRAD classification as stand-alone reporting systems. Both qualitative and LI-RADS version of reporting were almost equally specific and sensitive for the diagnosis of atypical or indeterminate HCC as stand-alone techniques. A quick and definitive histopathological evaluation of lesions which are suspicious or indeterminate for HCC on imaging should be undertaken during the course of evaluation of these patients, so as to expedite the management of HCC in this unique subset of patients.

References

[1] J. Ferlay, I. Soerjomataram, R. Dikshit, S. Eser, C. Mathers, Rebelo, et al., Cancer incidence and mortality worldwide: sources, methods and major patterns in GLOBOCAN 2012, Int. J. Cancer 136 (March (5)) (2015) E359–86.

[2] NCCN Clinical Practice Guidelines in Oncology on Hepatobiliary Cancer, (2016) Version http://www.nccn.org.

[3] R. Dhanasekaran, A. Limaye, R. Cabrera, Hepatocellular carcinoma: current trends in worldwide epidemiology, risk factors, diagnosis, and therapeutics, Hepat. Med. 4 (May) (2012) 19–37, https://doi.org/10.2147/HMER.S16316 PubMed PMID: 24367230; PubMed Central PMCID: PMC3846594.

[4] Surveillance Research Program, National Cancer Institute Fast Stats: An Interactive Tool for Access to SEER Cancer Statistics, (2011) Available from: http://seer.cancer.gov/faststatsAccessed August 15, 2011.

[5] M. Omata, A.L. Cheng, N. Kokudo, M. Kudo, J.M. Lee, J. Jia, et al., Asia-Pacific clinical practice guidelines on the management of hepatocellular carcinoma: a 2017 update, Hepatol. Int. 11 (4) (2017) 317–370, https://doi.org/10.1007/s12072-017-9799-9.

[6] T.H. Kim, J.H. Yoon, J.M. Lee, Emerging role of hepatobiliary magnetic resonance contrast media and contrast-enhanced ultrasound for noninvasive diagnosis of hepatocellular carcinoma: emphasis on recent updates in major guidelines, Korean J. Radiol. 20 (June (6)) (2019) 863–879, https://doi.org/10.3348/kjr.2018.0450 PubMed PMID: 31132813; PubMed Central PMCID: PMC6536788.

[7] K.M. Elsayes, A.Z. Kielar, V. Chernyak, A. Morshid, A. Furlan, W.R. Masch, et al., LI-RADS: a conceptual and historical review from its beginning to its recent integration into AASLD clinical practice guidance, J. Hepatocell. Carcinoma 6 (2019) 49–69, https://doi.org/10.2147/JHC.S186239 Published online 2019 Feb 5, PMCID: PMC6368120.

[8] J.H. Kim, I. Joo, J.M. Lee, Atypical appearance of hepatocellular carcinoma and its mimickers: how to solve challenging cases using gadoxetic acid-enhanced liver magnetic resonance imaging, Korean J. Radiol. 20 (July (7)) (2019) 1019–1041, https://doi.org/10.3348/kjr.2018.0636 Published online 2019 Jun 3, PMCID: PMC6609440.

[9] American College of Radiology, Liver Imaging Reporting and Data System Version, Accessed 15 Apr 2016, ACR Web site (2014) http://www.acr.org/Quality-Safety/Resources/LIRADS.

[10] EASL-EORTC clinical practice guidelines: management of hepatocellular carcinoma. European Association for Study of Liver. European Organisation for Research and Treatment of Cancer, Eur. J. Cancer 48 (March (5)) (2012) 599–641.

[11] K. Zakka, R. Jiang, O.B. Alese, W.L. Shaib, C. Wu, J.P. Wedd, et al., Clinical outcomes of rare hepatocellular carcinoma variants compared to pure hepatocellular carcinoma, J. Hepatocell. Carcinoma 6 (July) (2019) 119–129, https://doi.org/10.2147/JHC.S215235 PMID: 31413960; PMCID: PMC6660638.

[12] K.J. Fowler, T.A. Potretzke, T.A. Hope, E.A. Costa, S.R. Wilson, LI-RADS M (LR-M): definite or probable malignancy, not specific for hepatocellular carcinoma, Abdom. Radiol. (NY) 43 (2018) 149–157.

[13] M.E. Pittman, E.M. Brunt, Anatomic pathology of hepatocellular carcinoma: histopathology using classic and new diagnostic tools, Clin. Liver Dis. 19 (2015) 239–259.

[14] A. Quaglia, M.A. Jutand, A. Dhillon, et al., Classification tool for the systematic histological assessment of hepatocellular carcinoma, macroregenerative nodules, and dysplastic nodules in cirrhotic liver, World J. Gastroenterol. 11 (2005) 6262–6268.

[15] International Working Party, Terminology of nodular hepatocellular lesions, Hepatology 22 (1995) 983–993.

[16] International Consensus Group for Hepatocellular Neoplasia, Pathologic diagnosis of early hepatocellular carcinoma: a report of the international consensus group for hepatocellular neoplasia, Hepatology 49 (2009) 658–664.

[17] T. Roskams, M. Kojiro, Pathology of early hepatocellular carcinoma: conventional and molecular diagnosis, Semin. Liver Dis. 30 (2010) 17–25.

[18] S. Tremosini, A. Forner, L. Boix, R. Vilana, L. Bianchi, M. Reig, et al., Prospective validation of an immunohistochemical panel (glypican 3, heat shock protein 70 and glutamine synthetase) in liver biopsies for diagnosis of very early hepatocellular carcinoma, Gut 61 (2012) 1481–1487.

[19] L. Di Tommaso, G. Franchi, Y.N. Park, B. Fiamengo, A. Destro, E. Morenghi, et al., Diagnostic value of HSP70, glypican 3, and glutamine synthetase in hepatocellular nodules in cirrhosis, Hepatology 45 (2007) 725–734.

[20] M.S. Torbenson, Morphologic subtypes of hepatocellular carcinoma, Gastroenterol. Clin. N. Am. 46 (2017) 365–391.

[21] F.T. Bosman, F. Carneiro, R.H. Hruban, N.D. Theise, World Health Organization Classification of Tumours of the Digestive System, 4th ed, International Agency for Research on Cancer, World Health Organization, Lyon, 2010, pp. 205–216.

[22] J.A. Marrero, L.M. Kulik, C.B. Sirlin, A.X. Zhu, R.S. Finn, M.M. Abecassis, et al., Diagnosis, staging, and management of hepatocellular carcinoma: 2018 practice guidance by the American Association for the study of liver diseases, Clin. Liver Dis. 13 (1) (2019) 1, https://doi.org/10.1002/cld.802 PubMed Central PMCID: PMC6465784.

[23] S. Bota, F. Piscaglia, S. Marinelli, A. Pecorelli, E. Terzi, L. Bolondi, Comparison of international guidelines for noninvasive diagnosis of hepatocellular carcinoma, Liver Cancer 1 (3-4) (2012) 190–200, https://doi.org/10.1159/000343833 PubMed PMID: 24159584; PubMed Central PMCID: PMC3760457.

[24] A. Tang, A.G. Singal, D.G. Mitchell, E.M. Hecht, K.J. Fowler, L. Kulik, et al., Clin. Gastroenterol. Hepatol. 17 (7) (2019) 1228–1238 Epub 2018 Oct 1.

[25] A.G. Singal, A. Pillai, J. Tiro, Early detection, curative treatment, and survival rates for hepatocellular carcinoma surveillance in patients with cirrhosis: a meta-analysis, PLoS Med. 11 (4) (2014) e1001624.

[26] J. Bruix, M. Sherman, Management of hepatocellular carcinoma: an update. American Association for the study of liver diseases, Hepatology 53 (3) (2011) 1020–1022.

[27] A. Rastogi, Changing role of histopathology in the diagnosis and management of hepatocellular carcinoma, World J. Gastroenterol. 24 (35) (2018) 4000–4013, https://doi.org/10.3748/wjg.v24.i35.4000 PMC. PMCID: PMC6148422. PMID: 30254404..

[28] A. Forner, R. Vilana, C. Ayuso, L. Bianchi, M. Solé, J.R. Ayuso, et al., Diagnosis of hepatic nodules 20 mm or smaller in cirrhosis: prospective validation of the non-invasive diagnostic criteria for hepatocellular carcinoma, Hepatology 47 (1) (2008) 97–104, https://doi.org/10.1002/hep.21966 PMID:18069697.

[29] M.W. Lai, Y.D. Chu, C.L. Lin, R.N. Chien, T.S. Yeh, T.L. Pan, et al., Is there a sex

difference in postoperative prognosis of hepatocellular carcinoma? BMC Cancer 19 (1) (2019) 250, https://doi.org/10.1186/s12885-019-5453-3 PMID: 30894157; PMCID: PMC6425676.

[30] Pathologic diagnosis of early hepatocellular carcinoma: a report of the international consensus group for hepatocellular neoplasia. International Consensus Group for Hepatocellular Neoplasia. The International Consensus Group for Hepatocellular Neoplasia, Hepatology 49 (2) (2009) 658–664, https://doi.org/10.1002/hep.22709 PMID:19177576.

[31] K.W. Gu, Y.K. Kim, J.H. Min, S.Y. Ha, W.K. Jeong, Imaging features of hepatic sarcomatous carcinoma on computed tomography and gadoxetic acid-enhanced magnetic resonance imaging, Abdom. Radiol. (NY) 42 (2017) 1424–1433.

[32] N. Zhang, Y. Li, M. Zhao, X. Chang, F. Tian, Q. Qu, et al., Sarcomatous intrahepatic cholangiocarcinoma: case report and literature review, Medicine (Baltimore) 97 (39) (2018) e12549, https://doi.org/10.1097/MD.0000000000012549 Erratum in: Medicine (Baltimore). 2018 Oct;97(42):e12951. PMID: 30278551; PMCID: PMC6181610.

[33] J.H. Kim, I. Joo, J.M. Lee, Atypical appearance of hepatocellular carcinoma and its mimickers: how to solve challenging cases using gadoxetic acid-enhanced liver magnetic resonance imaging, Korean J. Radiol. 20 (7) (2019) 1019–1041, https://doi.org/10.3348/kjr.2018.0636 PMID: 31270973; PMCID: PMC6609440.

[34] S.H. Liao, T.H. Su, Y.M. Jeng, P.C. Liang, D.S. Chen, C.H. Chen, et al., Clinical manifestations and outcomes of patients with sarcomatoid hepatocellular carcinoma, Hepatology 69 (1) (2019) 209–221, https://doi.org/10.1002/hep.30162 PMID: 30014620.

[35] F.H. Wu, C.H. Shen, S.C. Luo, J.I. Hwang, W.S. Chao, H.Z. Yeh, et al., Liver resection for hepatocellular carcinoma in oldest old patients, World J. Surg. Oncol. 17 (1) (2019) 1, https://doi.org/10.1186/s12957-018-1541-0 PMID: 30606220; PMCID: PMC6317186.

[36] A. Paisant, V. Vilgrain, J. Riou, F. Oberti, O. Sutter, V. Laurent, et al., Comparison of extracellular and hepatobiliary MR contrast agents for the diagnosis of small HCCs, J. Hepatol. (2019), https://doi.org/10.1016/j.jhep.2019.12.011 S0168-8278(19) 30725-31, Epub ahead of print]. PMID: 31870951.

[37] S.M. Lee, J.M. Lee, S.J. Ahn, H.J. Kang, H.K. Yang, J.H. Yoon, LI-RADS Version 2017 versus Version 2018: diagnosis of hepatocellular carcinoma on gadoxetate disodium-enhanced MRI, Radiology 292 (3) (2019) 655–663, https://doi.org/10.1148/radiol.2019182867 Epub 2019 Jul 16. PubMed PMID: 31310175.

[38] S.K. Shin, Y.S. Kim, S.J. Choi, Y.S. Shim, D.H. Jung, O.S. Kwon, et al., Characterization of small (≤3 cm) hepatic lesions with atypical enhancement feature and hypointensity in hepatobiliary phase of gadoxetic acid-enhanced MRI in cirrhosis: a STARD-compliant article, Medicine (Baltimore) 96 (29) (2017) e7278,

https://doi.org/10.1097/MD.0000000000007278 PubMed PMID: 28723741; PubMed Central PMCID: PMC5521881.

[39] I. Kim, M.J. Kim, Histologic characteristics of hepatocellular carcinomas showing atypical enhancement patterns on 4-phase MDCT examination, Korean J. Radiol. 13 (5) (2012) 586–593, https://doi.org/10.3348/kjr.2012.13.5.586 Epub 2012 Aug 28. PubMed PMID: 22977326; PubMed Central PMCID: PMC3435856.

[40] P. Hytiroglou, Y.N. Park, G. Krinsky, N.D. Theise, Hepatic precancerous lesions and small hepatocellular carcinoma, Gastroenterol. Clin. North Am. 36 (4) (2007) 867–887, https://doi.org/10.1016/j.gtc.2007.08.010 vii. PMID: 17996795..

[41] S. Monzawa, K. Omata, N. Shimazu, A. Yagawa, K. Hosoda, T. Araki, Well-differentiated hepatocellular carcinoma: findings of US, CT, and MR imaging, Abdom. Imaging 24 (4) (1999) 392–397, https://doi.org/10.1007/s002619900521 PMID:10390564.

[42] J. Shin, J.Y.J. Yu JH, M.H. Chae, C.H. Yoon, J.W. Lee, Comparison of survival outcomes of alcohol-related hepatocellular carcinoma with or without liver cirrhosis; a ten-year experience, Medicine (Baltimore) 98 (47) (2019) e18020, , https://doi.org/10.1097/MD.0000000000018020 PMID: 31764818.

[43] L.A. Balaceanu, Biomarkers vs imaging in the early detection of hepatocellular carcinoma and prognosis, World J. Clin. Cases 7 (12) (2019) 1367–1382, https://doi.org/10.12998/wjcc.v7.i12.1367 PMID: 31363465; PMCID: PMC6656675].

[44] M.I.A. Edoo, V.K. Chutturghoon, G.K. Wusu-Ansah, H. Zhu, T.Y. Zhen, H.Y. Xie, et al., Serum biomarkers AFP, CEA and CA19-9 combined detection for early diagnosis of hepatocellular carcinoma, Iran. J. Public Health 48 (2) (2019) 314–322 PMID:31205886.

[45] European Association for the Study of the Liver, European Association for the Study of the Liver, EASL clinical practice guidelines: management of hepatocellular carcinoma, J. Hepatol. 69 (2018) 182–236, https://doi.org/10.1016/j.jhep.2018.03.019 PMID: 29628281.

[46] K.W. Burak, M. Sherman, Hepatocellular carcinoma: consensus, controversies and future directions. A report from the Canadian Association for the study of the liver hepatocellular carcinoma meeting, Can. J. Gastroenterol. Hepatol. 29 (2015) 178–184.

[47] T.J. Fraum, R. Tsai, E. Rohe, D.R. Ludwig, A. Salter, I. Nalbantoglu, et al., Differentiation of hepatocellular carcinoma from other hepatic malignancies in patients at risk: diagnostic performance of the liver imaging reporting and data system version 2014, Radiology 286 (1) (2018) 158–172.

[48] M. Renzulli, A. Clemente, S. Brocchi, M. Milandri, V. Lucidi, R. Vukotic, et al., LI-RADS: a great opportunity not to be missed, Eur. J. Gastroenterol. Hepatol. 31 (3) (2019) 283–288, https://doi.org/10.1097/MEG.0000000000001269 PMID: 30234643.